Journal of Power Sources 481 (2021) 228804

Contents lists available at ScienceDirect

Journal of Power Sources

journal homepage: www.elsevier.com/locate/jpowsour

Perspective

Redox flow batteries: Status and perspective towards sustainable stationary energy storage

Eduardo Sánchez-Díez [a,*], Edgar Ventosa [b,c], Massimo Guarnieri [d], Andrea Trovò [d], Cristina Flox [e], Rebeca Marcilla [f], Francesca Soavi [g], Petr Mazur [h], Estibaliz Aranzabe [i], Raquel Ferret [a,**]

[a] Centre for Cooperative Research on Alternative Energies (CIC EnergiGUNE), Basque Research and Technology Alliance (BRTA), Alava Technology Park, Albert Einstein 48, 01510, Vitoria-Gasteiz, Spain
[b] Department of Chemistry, University of Burgos, Pza. Misael Bañuelos s/n, E-09001, Burgos, Spain
[c] International Research Centre in Critical Raw Materials-ICCRAM, University of Burgos, Plaza Misael Bañuelos s/n, E-09001, Burgos, Spain
[d] Department of Industrial Engineering, University of Padua, Via Gradenigo 6a, 35131, Padova, Italy
[e] Department of Chemistry and Materials Science, School of Chemical Engineering, Aalto University, 16100, FI-00076, Aalto, Finland
[f] Electrochemical Processes Unit, IMDEA Energy, Avda. Ramón de la Sagra 3, 28935, Móstoles, Spain
[g] Department of Chemistry "Giacomo Ciamician", Alma Mater Studiorum Universitá di Bologna, Via Selmi 2, 40126, Bologna, Italy
[h] New Technologies – Research Centre, University of West Bohemia Pilsen, Univerzitni 8, 301 00, Plzen, Czech Republic
[i] Surface Chemistry and Nanotechnologies Unit, TEKNIKER, Iñaki Goenaga 5, 20600, Eibar, Spain

HIGHLIGHTS

- Redox-flow batteries are moving forward to sustainable stationary storage.
- Focus for RFBs is put on durability and cost targets.
- VRFBs are leading in terms of performance and market permeation.
- Alternative technologies are mainly based on low-cost abundant active materials.
- Membraneless and semisolid RFBs go beyond current conceptual limitations.

GRAPHICAL ABSTRACT

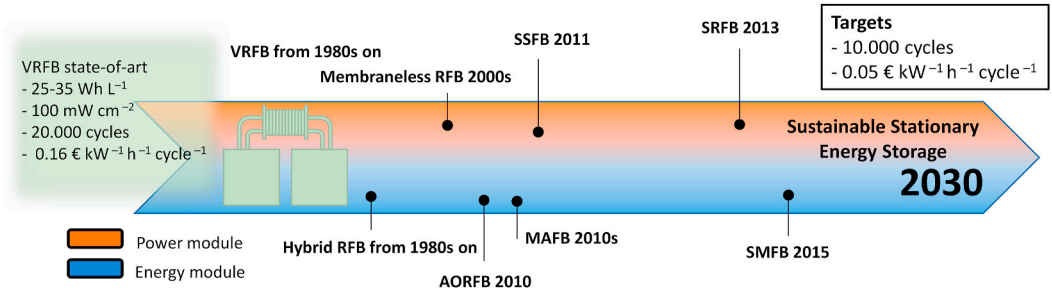

ARTICLE INFO

Keywords:
Electrochemical energy storage
Stationary energy storage
Redox-flow batteries
Sustainable energy

ABSTRACT

Redox-flow batteries, based on their particular ability to decouple power and energy, stand as prime candidates for cost-effective stationary storage, particularly in the case of long discharges and long storage times. Integration of renewables and subsequent need for energy storage is promoting effort on the development of mature and emerging redox-flow technologies. This review aims at providing a critical analysis of redox-flow technologies that can potentially fulfill cost requirements and enable large scale storage, mainly aqueous based systems. A comprehensive overview of the status of those technologies, including advantages and weaknesses, is presented.

* Corresponding author.
** Corresponding author.
E-mail addresses: esanchez@cicenergigune.com (E. Sánchez-Díez), eventosa@ubu.es (E. Ventosa), massimo.guarnieri@unipd.it (M. Guarnieri), andrea.trovo@unipd.it (A. Trovò), cristina.flox@aalto.fi (C. Flox), rebeca.marcilla@imdea.org (R. Marcilla), francesca.soavi@unibo.it (F. Soavi), mazurp@ntc.zcu.cz (P. Mazur), earanzabe@tekniker.es (E. Aranzabe), rferret@cicenergigune.com (R. Ferret).

https://doi.org/10.1016/j.jpowsour.2020.228804
Received 15 June 2020; Received in revised form 31 July 2020; Accepted 14 August 2020
Available online 16 September 2020

Compiled data on the market permeability, performance and cost should serve, together with the perspective included, to understand the different strategies to reach the successful implementation, from component development to innovative designs.

1. Introduction

In the current scenario of energy transition, there is a need for efficient, safe and affordable batteries as a key technology to facilitate the ambitious goals set by the European Commission in the recently launched Green Deal [1]. The bloom of renewable energies, in an attempt to confront climate change, requires stationary electrochemical energy storage [2] for effective integration of sustainably generated electrical energy. Indeed, the inclusion of 20% renewables might be sufficient to destabilize the grid due to their intermittent nature [3].

The global Energy Transition scenario implies large scale considerations when defining a solution. Lithium Ion Batteries (LIBs) are ubiquitous in our society and dominate the energy storage market powering portable devices, EVs and even smart grid facilities. In 2019, 8.8 GWh of LIB capacity were installed for stationary energy storage vs. 0.25 GWh of Redox Flow Batteries (RFBs). However, its high maintenance cost and safety limitations, in addition to the limited availability of lithium, note the interest in developing alternatives to efficiently store energy.

Large-scale grid storage requires long life-low cost batteries, considering both cyclability, calendar life, and round-trip efficiency. Installation and maintenance costs are still the main barriers for penetration of storage on the grid. Thus, clear targets have been set in the SET Plan, for stationary energy storage in terms of cost (0.05 € $kW^{-1}h^{-1}$ $cycle^{-1}$) and durability (10,000 cycles and 20 years lifetime) for 2030 [4].

RFBs have emerged as relevant candidates to address the sustainable energy generation. Their unique capability to decouple power and energy based on their particular architecture results in advantages such as: flexible modular design and operation, excellent scalability, moderate maintenance costs and long-life cycling. Thus, the system consists of three main components: energy storage tanks, stack of electrochemical cells and the flow system. Fig. 1 shows an archetypical redox flow battery, e.g. Vanadium redox flow battery (VRB or VRFB).

The energy storage proceeds as follows: 1) active species are contained in the tanks as a solution with a certain energy density, 2) the solution, defined as electrolyte, is pumped into the stack, where the electrochemical conversion takes place and collected back in the tanks. The size of the stack defines the power of the system whilst the amount of electrolyte stored in the tanks states the total energy.

High round trip efficiency (RTE), Depth of discharge (DoD), fast responsiveness and negligible environmental impact (e.g. aqueous RFBs) are other key features for the technology successful deployment. Power and energy density limitations in comparison to other technologies such as LIBs are generally overcome by the more cost-effective scalability.

Alternatively to the standard RFBs, systems comprising at least one solid electroactive material that is deposited or stripped within the stack, have been widely explored (e.g. Zn based RFBs). Those, so called hybrid RFBs, differ from the previous type in their capability to decouple power and energy, which is limited by the solid electrode (Fig. 2). Hereafter, RFBs that store electroactive material only in outer tanks and flown through the cell in its reduced and oxidized states will be termed pure flow RFBs.

Thus, both pure flow RFBs and their hybrid counterparts have been successfully deployed, where VRFB and zinc-bromine redox flow batteries (ZBFBs) can be clearly defined as state-of-the-art (SoA) for the technology. Nevertheless, those have still a long way to go to meet the targets defined by energy institutions, and a new bunch of RFB systems is irrupting to oust VRFBs and show up as real alternatives to reach the market (Fig. 3).

Excellent reviews have already covered in depth the chemistry, components and performance of RFBs [5–9]. This review does not

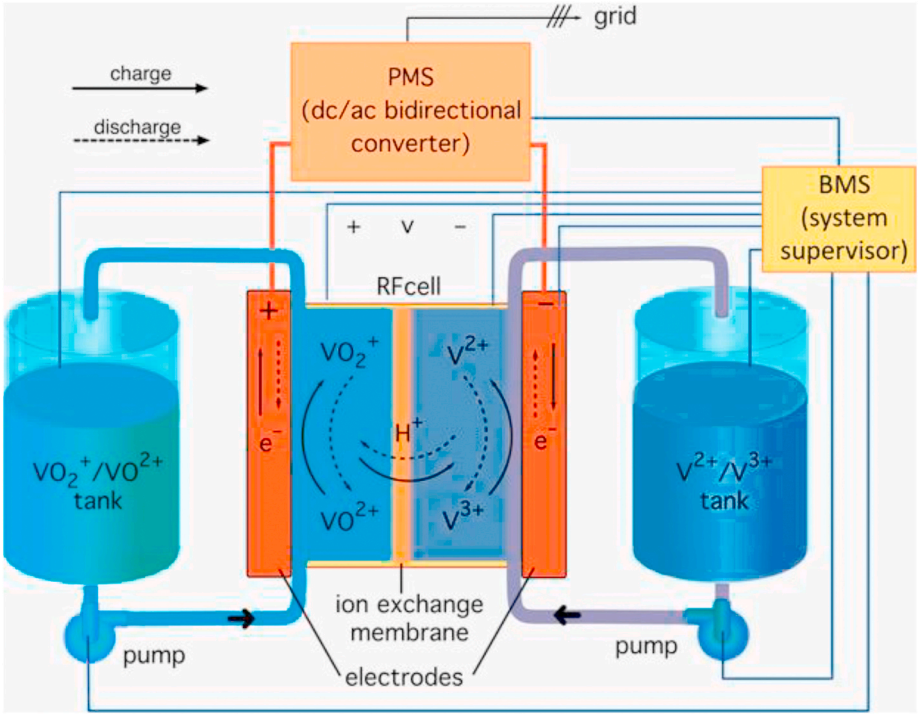

Fig. 1. Scheme of a kW-class VRFB system. A single-cell electrochemical converter is shown.

intend to cover detailed information on components, though in many cases the chemistry of the electrolyte, as the main component, will serve to distinguish and classify developed RFB technologies. Equally, no system integration aspects will be detailed due to the lack of maturity of the presented alternatives. The overall purpose of this review is to examine technologies that can potentially fulfill cost requirements and enable large scale storage. In that sense, subsequent sections will be focused, with limited exceptions, on aqueous systems based on their technical and economic advantages. After a short overview of the **State of the art of industrialized flow batteries** for both pure flow and hybrid RFBs, the status of less mature technologies will be described in sections 3-5. Following the classification defined in section 2, **Alternatives for pure flow/flow batteries** and **Alternatives for hybrid flow/non-flow batteries** will be covered separately in sections 3 and 4 respectively. Section 5 is devoted to recent and unexplored RFBs and/or disruptive technologies that go beyond standard RFB configuration as defined in this section, i.e. solar redox-flow batteries.

2. State of the art of industrialized flow batteries

2.1. Vanadium redox flow battery – VRFB

In the last few decades, RFBs have been studied and developed based on different chemistries. Among them, the most successful is the all-vanadium RFB, which has reached effective commercial fruition starting in the 1980s [10]. The Vanitec website lists 26 companies as producers of this technology [11] and several plants have been installed globally [12]. Among the largest are the Minami Hayakita Substation in Japan, rated 15 MW and 60 MWh and built by Sumitomo Electric Ind. for Hokkaido Electric Power Inc. in 2015, and the energy storage station at Fraunhofer ICT in Pfinztal, Germany, rated 2 MW and 20 MWh and commissioned in 2019, while UniEnergy Technologies, US-WA, has installed a number of systems rated 2 MW and 8 MWh. The largest project so far is the 200 MW 800 MWh Storage Station designed by Rongke Power of China. When completed it will be by far the largest electrochemical energy storage plant in the world.

A VRFB works as a standard RFB with the positive and negative electrolytic solutions stored in two tanks from where they are circulated to the electrochemical cells by means of two pumps (Fig. 1). Thanks to the ability of vanadium to exist in solution in four different oxidation states, vanadium ions are used at both compartments, namely vanadium IV-V (tetravalent-pentavalent VO^{2+} and VO_2^+) in the positive electrolyte and vanadium II-III (bivalent-trivalent V^{2+} and V^{3+}) in the negative electrolyte. The electrochemical half-reactions produced by these solutions in the cells are:

$$\text{positive electrode: } VO_2^+ + 2H^+ + e^- \underset{\text{charge}}{\overset{\text{discharge}}{\rightleftharpoons}} VO^{2+} + H_2O \quad E_{0+} = +1.00\,V \text{ vs. } SHE$$

$$\text{negative electrode: } V^{2+} \underset{\text{charge}}{\overset{\text{discharge}}{\rightleftharpoons}} V^{3+} + e^- \quad E_{0-} = -0.26\,V \text{ vs. } SHE \tag{1}$$

The corresponding standard cell voltage is $E_0 = 1.26$ V at 25 °C and 50% SoC, but real cells exhibit $E_0' = 1.4$ V, due to side effects, mainly the Donnan potential appearing at the membrane surfaces [13]. Based on Nernst's equation (2), the OCV varies with the SoC as

$$V_{oc} = E_O^{'} + \frac{KT}{F} in \frac{SOC_+ SOC_-}{(1 - SOC_+)(1 - SOC_+)} \tag{2}$$

where K is the universal gas constant, F the Faraday constant and T the absolute temperature. Consequently, the operative OCV ranges from 1.1 V to 1.6 V. Typically, 1.6–1.7 M vanadium ions are dissolved in a sulfuric acid solution with a total sulfate concentration of ~5 M, but up to 2.5 M [14] and even 3 M active material concentrations [15] were successfully experimented using proper acid mixes and precipitation inhibitors. Correspondingly, stored energy density ranges as 25–35 Wh L^{-1}, i.e. much less than LIBs, which are capable of 250 Wh L^{-1} and more. Using the same metal in both electrolytes prevents cross-contamination, allowing for a lifespan longer than any other solid-state or flow battery, i.e. typically 15.000–20.000 charge/discharge cycles as compared to the top figure of 5.000 typical of other batteries.

Several cells are connected in series to form a stack, so as to produce total voltages of some tens of volts, whereas the cell cross sectional area

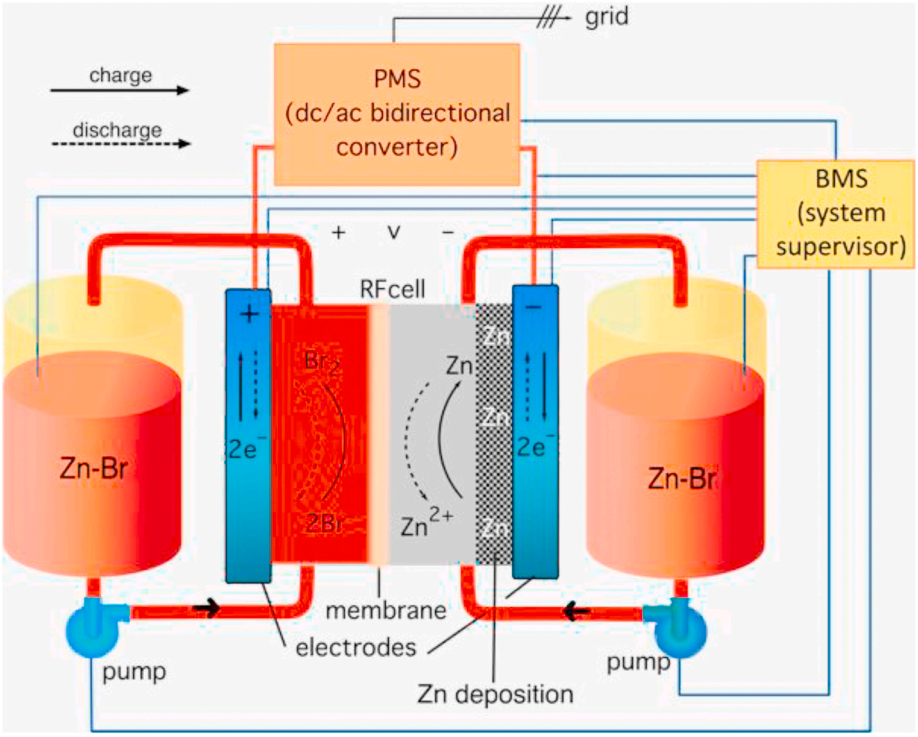

Fig. 2. Scheme of a kW-class hybrid Zn–Br FB system. A single-cell electrochemical converter is shown.

defines the stack current. Two architectures are used to flow the electrolytic solutions in the cell electrodes. In the "flow-by" design, the bipolar plates interposed between adjacent cells have flow channels on each face, to distribute the electrolytes into thin electrodes. In the "flow-through" design bipolar plates have flat faces and electrolytes percolate transversally from one side to opposite one of thicker electrodes.

In such a well-established technology, efforts are devoted to improve efficiency and increase defined current and power densities. The typical current density of commercial VRBs is in the order of 80–100 mA cm^{-2} and correspondingly the power density barely reaches 100 mW cm^{-2}, i.e. much less than equivalent proton exchange membrane fuel cells (PEMFCs). Active cell areas of 6000 cm^2 and over have been developed for producing currents of some hundreds of amperes. However, current density up to 1.5 A cm^{-2} and power density of 1.1 W cm^{-2} were experimented in small tests cell [16,17] and kW-class pilot systems have been built capable of 665 mA cm^{-2} and 370 mW cm^{-2} [18]. Round trip efficiencies over 85–90% have been tested in small single cells [19,20], and up to 57–75% in kW-class pilot systems, which are burdened by hydraulic losses and shunt currents, by means of dynamically optimized electrolyte flows [21,22].

Thanks to the fast electrochemical kinetics, the response time is very short, in the order of a millisecond, if the electrodes are kept full of electrolytes and pumps in standby promptly take over. This allows VRFBs to respond immediately to surge power demand from the grid, coping with power quality grid services such as sag compensation and frequency regulation [23,24]. The electrolytes which remain inside the electrodes in standby also allow overcurrents of 150% and more in the first few milliseconds after insertion, before concentration gradients take over [18].

During charge/discharge, the cell voltage differs from the OCV due to activation losses η_a, concentration (i.e. mass transport) losses η_c, and ohmic losses $R_i I$ (equation (3)):

$$V = V_{oc} - n_o - n_c - R_i I \tag{3}$$

Activation losses have typically a minor effect, if high-performing materials are used in the electrodes and mass transport losses remain low also at high current density if adequate electrolyte flow rates are applied (i.e. flow factors higher than 7.5) [22,25]. Thus, the voltage drop mainly depends on the ohmic losses, in a well-designed and properly operated stack, so that reducing the internal cell resistance is crucial to increase the performance [26].

As other batteries, VRFBs need a bidirectional d.c./a.c. inverter, i.e. the Power Management System (PMS), to interface the grid. This must operate at variable d.c. voltage while assuring high efficiency, that call for an advanced design [27]. Control functions, e.g. electrolyte flow rate, are performed by the system supervisor, that is often called Battery Management System (BMS), although being quite different from the BMS of a solid-state battery [28]. The Levelized Costs of Storage (LCOS), i.e. the ratio of the total investment and the total energy managed in the system lifetime also accounting for the system efficiency, has been indicated in 0.18 € $kW\,h^{-1}$ $cycle^{-1}$ [29].

Present research aims at electrolytes capable of increased -active material concentrations and energy density [30], membranes with higher proton conductivity and lower ions crossover [31], porous electrodes capable of better hydraulic performance [32]. Nevertheless, major issues remain. Low values of energy density make a VRFB system much bulkier than an equivalent Li-ion system. Vanadium is classified as a strategic material, being mined in few non-European nations all over the world, and scarcity or limited availability lead to highly volatile price/supply of V_2O_5 [33–35]. On the other hand, no vanadium consumption occurs in VRFBs, so that it can be recycled at will in future plants [36]. In this regards, electrolyte leasing has been proposed to decrease costs. A more economics-based approach aims for large scale devices and vertical integrated company models, e.g. Bushveld Energy (South Africa) [37].

2.2. Zinc–bromine flow battery – ZBFB

Several zinc-based chemistries have been proposed for flow or hybrid batteries, some of which have been scaled-up into industrial systems [38]. They use a zinc negative electrode and exhibit an operating OCV around 1.58 V [39]. Among them, the zinc-bromine flow battery (ZBFB) is the most investigated and successfully commercialized. ZBB technologies (now Ensync Energy systems, US) manufactured a 2 MW/2 MWh system for load leveling service in 2004 [40]. Redflow Ltd. (Australia) and Primus Inc. (US) are producing Zn–Br RFBs for load leveling service with stored energies up to 600 kWh since 2000. In the 1980s, ZBFBs were experimented for EVs. In the 1990s, electric vehicles powered with 35 kWh Zn–Br batteries were tested at the University of California, by Toyota Motors (Japan) in the model EV-3036 (7 kWh, 106 V) [40], and by Fiat (Italy) in a Panda city car (18 kWh, 72 V, 250 A h).

This battery is commonly referred to as the most representative example of hybrid flow batteries. Zinc bromide aqueous solutions are used as electrolyte stored in both tanks and pumped into the stack. Bromine is always dissolved, whereas zinc is solid in a charged battery and is dissolved to Zn^{2+} is a discharged one. This solid zinc is deposited onto the negative carbon electrode, thus conferring the hybrid nature to the battery (Fig. 2). In this process, dendrite can grow and after extended cycling can cause channel blockage and cell failure. The electrochemical half-reactions are:

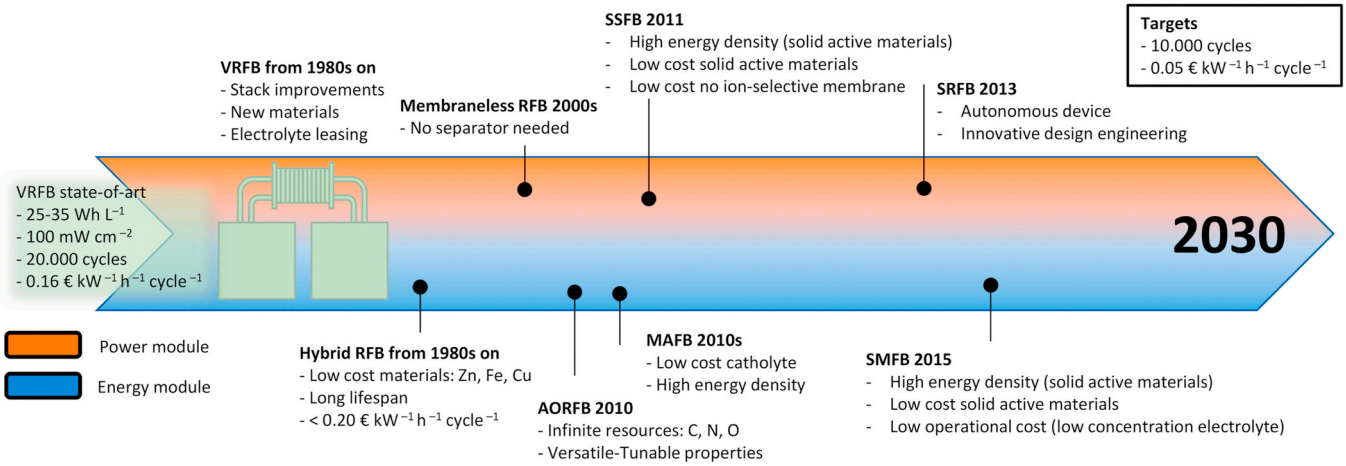

Fig. 3. Scheme of state-of-the-art of RFBs. Timeline including industrialized and innovative technologies and description of strategies to achieve low cost batteries.

$$\begin{aligned} &positive\ electrode: \quad Br_2 + 2e^- \underset{charge}{\overset{discharge}{\rightleftharpoons}} 2Br^- \quad E_{0+} = +1.09 \ V\ vs.\ SHE \\ &negative\ electrode: \quad Zn^0 \underset{charge}{\overset{discharge}{\rightleftharpoons}} Zn^{2+} + 2e^- \quad E_{0-} = -0.76 \ V\ vs.\ SHE \end{aligned} \tag{4}$$

The cell exhibits a high standard cell voltage of 1.85 V and a high theoretical specific energy of 440 Wh kg^{-1}, but both figures are lower in the case of the real systems, e.g. commercial systems present specific energy of 60—85 Wh kg^{-1} [41]. In addition, these systems present in general quite low current densities, typically few tens of mA cm^{-2} [42]. ZBFB have no cycle-life limitations because the electrolytes do not suffer aging effects: lifetimes of 11–14 years are commercially proposed. ZBFB pilot systems are capable of charge/discharge durations up to 10 h [43], a performance comparable to commercial VRFBs and can operate at current densities up to 80 mA cm^{-2}, with energy efficiencies around 80% [44].

During operation, bromine is sequestered and stored in an oily phase that remains separated from the aqueous phase of the electrolyte due to the different specific gravity of the complexed phase. ZBFBs offer 100% DoD capability, but they need to be fully discharged every few days to prevent dendrites growth from short-circuiting the separator and also need to be periodically shorted at the terminals while running the electrolyte pump, to fully remove zinc from battery plates [45].

Even though zinc and bromine are low-cost materials, ZBFB systems are not cheaper than an equivalent VRFB, due to expensive sequestering/complexing agents needed to avoid toxic bromine vapor emissions. LCOS comparable to those of VRFBs have been indicated for standard ZBFB <0.20 € $kW^{-1}h^{-1}$ $cycle^{-1}$ [46].

3. Alternatives for pure flow/flow batteries

The maturity level of VRFBs has resulted in the deployment of this technology all over the world and research is on a good track to improve the performance of this system. However, the aforementioned intrinsic limitations of standard VRFBs and the uncertainty on the availability of vanadium to meet the increasing global demand, promote a broad body of research for several different alternatives.

As an approach to face the problems inherent to current state of the art in pure flow systems, different strategies, including new redox chemistries and new cell configurations, have been sounded out. Main focus is to decrease system cost by either improving current electrolytes, e.g. new formulations, or directly obtaining new efficient and safe low-cost electrolytes to replace vanadium, avoiding currently employed expensive membranes and increasing the system energy density by different means. Beyond the innovation on the components, research has been devoted to surpassing conceptual limitations of redox flow batteries. New technologies capable of dodging problems as energy density or resistive physical barriers in the cell are presented and those are to face other challenges to reach market and succeed.

3.1. Alternative aqueous inorganic pure flow batteries

Back to the beginning, RFBs were conceived based on the use of metal redox couples as active material for the electrolyte. High stability at different oxidation states and good redox kinetics are identified as key parameters for the success of metal ions as redox active materials. Some of those, although proposed several decades ago, are still subject of study (V, Fe, Ce). In addition, the use of inorganic species has been extended to several other compounds (e.g. halides, sulfides, hydrogen or oxygen) that have been coupled with metal ions or employed independently as in the case of hydrogen-bromine flow batteries (HBFBs). Some of the technologies that aim to dare all-vanadium's supremacy are discussed in this section.

3.1.1. Vanadium–oxygen redox flow battery - VORFB

Vanadium-oxygen RFBs have been derived from VRFBs by replacing the positive half-cell with an air electrode, with the advantages that: the energy density is increased, the needed quantity of vanadium is reduced, V(V) is avoided together with the risk of its precipitation at high temperature. Only tested at small scale, so far, these cells are often referred to as V/O fuel cells (VOFCs), due to the lack of reversibility in the positive electrode. This issue can be overcome by adding an electrolyzer, provided with special catalysts, that operated as a reverse H_2/O_2 fuel cells. A cell based on the reaction of vanadium and oxygen was first proposed in a patent by Kaneko et al., in 1992, then dubbed a redox battery [47] producing the following half-reactions

$$\begin{aligned} &positive\ electrode: \quad O_2 + 4e^- + 4H^+ \underset{charge}{\overset{discharge}{\rightleftharpoons}} 2H_2O \ E_{0+} = +1.23 \ V\ vs.\ SHE \\ &negative\ electrode: \quad V^{2+} \underset{charge}{\overset{discharge}{\rightleftharpoons}} V^{3+} + e^- \quad E_{0-} = -0.26 \ V\ vs.\ SHE \end{aligned} \tag{5}$$

Atmospheric or pure oxygen reduction is promoted by a catalyst. The standard cell voltage is 1.49 V and the theoretical energy density is more than doubled with respect to VRFB. Current densities up to 10 mA cm^{-2} could be obtained.

Later on, the VOFC concept was extensively investigated by Menictas and Skyllas-Kazacos, at UNSW, who used 1.8 M V(II) in 5 M H_2SO_4 at the negative electrode and gaseous oxygen at the positive electrode [48]. They used a 5-cell VOFC provided with different types of membranes (Nafion 112 and Nafion 117) and air electrode assemblies (i.e. different membrane electrode assemblies – MEAs) for investigating the performance over a range of temperatures. The biggest challenge was MEA swelling (expansion) and consequent catalyst layer dissolution [10]. After limiting this effect, the 5-cell stack could be operated over a period of 100 h, OCVs up to 1.41 V and current densities up to 40 mA cm^{-2} were achieved. They also observed a marked benefit in using preheated oxygen.

In 2010 Noack et al. published an experimental comparison between a VOFC and a VRFB [49]. They used a 1.6 M VSO_4 solution in 2 M H_2SO_4. The VOFC maximum discharge power density was 30 mW cm^{-2}. Hosseiny et al. reported a VO cell that they dubbed vanadium-air redox-flow battery (VARFB) and used two MEAs, one for charging and one for discharging, with titanium/iridium catalyst and platinum/carbon catalyst, respectively [50]. The negative electrolyte was a 2 M V(II)/V(III) solution in 3 M H_2SO_4 and the charge and discharge current density was 2.4 mA cm^{-2}. Due to the absence of V(V), and therefore precipitation, they operated the VARFB with 4 M V(II) and V(III) at temperature as high as 80 °C without damaging the membrane. An energy efficiency of 45.7% was achieved. However, a reduction of the OCV in time was observed, due to self-discharge and possibly to oxygen crossover.

In 2011 Palminteri et al. observed that the diffusion of the V(II) solution into the positive compartment caused a strong hydrogen evolution in the Pt-based MEA. In addition, the detachment of the catalyst layer caused a considerable decrease of the battery power density [51]. To counteract this issue, Noack et al. developed a cell with two membranes and an intermediate compartment [52], where diffusing V(II) was oxidized to V(III), thus preventing hydrogen formation at the Pt particles of the MEA.

Recently, Risbud et al. published a study on a VOFCs 30-cm^2 single cell [53]. They tested V(II) concentrations up to 3.6 M in 5 M H_2SO_4 by using precipitation inhibitors. The effect of the catalysts on both electrodes, mainly for the positive one, were evaluated. OCVs up to 1.35 V–1.4 V were achieved at 80 °C with Pt/C positive electrodes. By using a solution of 3.6 M V(II) in 6–8 M H_2SO_4 at 50 °C and a commercial Pt MEA, a power density of 34.5 mW cm^{-2} was obtained at 50 mA cm^{-2} with an energy efficiency of 46%. Oxygen transport, related to water formation from the electrochemical half-reaction, was observed and counteracted, allowing to achieve a maximum current density 100 mA cm^{-2}. V(II) and oxygen crossover were also observed to affect performance.

At present, the challenges of VORFBs are long-term stability, high

concentration of the V(III)/V(II) solutions, efficient water management at the cathode, and higher current, energy and power densities. When, and if, developed at an industrial scale, the cost of this battery will highly depend on trade-off between the cost of saved vanadium at the positive compartment and the cost of catalysts employed at the positive electrode.

3.1.2. Vanadium–bromine redox flow battery – VBFB

The vanadium/bromine (V–Br) battery (or 2nd generation VRFB, i.e. G2 V/Br) aims at overcoming the limited energy density on VRFBs (in this context, 1st generation, G1 VFB) while enhancing its advantages. This chemistry has been tested on the small scale, so far. After, registering the first patent in 2001, Skyllas Kazacos was the main contributor to the development of VBFBs in the following years [54,55]. The electrochemical reactions are:

$$\begin{aligned} &positive\ electrode: Cl Br_2^- + 2e^- \underset{charge}{\overset{discharge}{\rightleftharpoons}} 2Br^- + Cl^- \quad E_{0+} = +1.04\ V\ vs.\ SHE \\ &negative\ electrode: V Br_2 + Br^- \underset{charge}{\overset{discharge}{\rightleftharpoons}} V Br_3 + e^- \quad E_{0-} = -0.25\ V\ vs.\ SHE \end{aligned} \tag{6}$$

Main features of VBFBs are:

- It employs a vanadium bromide solution in both half-cells, thus avoiding cross-contamination.
- The high solubility of V/Br, allows to increase the concentration of vanadium in solution to 3–4 M, allowing for energy densities up to 50–70 Wh·L^{-1}.
- The high solubility of V/Br allows for lower temperature operations.
- The high temperature limit is not affected by the precipitation of V (V), that is absent.

A variation of the vanadium-bromide cell consists of the vanadium/polyhalide cell, in which polyhalide, resulting from the interaction between halogen molecules and Br_2Cl^- or Cl_2Br^-, offers higher oxidation potential. Skyllas-Kazacos filed a number of patents on these concepts [56–58]. Research carried out by UNSW and V-Fuel Pty Ltd in the period 2005–2010 allowed to select highly stable, low-cost membranes and electrode materials.

Typical electrolytes consist of 2–2.6 M $V^{3.5+}$ in a mixture of 6.4–7.5 M HBr plus 1.5–2 M HCl (35–45 Wh L^{-1}) [59]. Single cell energy efficiency, (i.e. coulombic efficiency multiplied by voltage efficiency excluding hydraulic losses and PMS losses) as high as 80% was found in a small 25 cm^2 single cell at a current density of 25 mA cm^{-2} [54]. Later on, a small vanadium/polyhalide cell was tested with charge/discharge operation at current density of 20 mA cm^{-2} in small single cell obtaining coulombic and voltage efficiencies of 83% and 80%, respectively, i.e. an energy efficiency of 66% [60].

Some complexing agents have been studied and successfully tested to prevent the emissions of toxic bromine vapor, e.g. quaternary ammonium bromides (MEM-Br, MEP-Br, TBA-Br) [61]. MEM and MEP can reduce Br_2 vapors effectively, but increase the membrane resistance. On the other hand, these complexing agents do not affect the kinetics of Br_2/Br^-, that depends on mass transport. However, they are too expensive for commercial application, at present. More complexing agents have been proposed recently, also capable of enhancing the electrochemical reversibility by improving the diffusion coefficient of vanadium [62]. Yet, the economic viability of this solution is to be demonstrated on an industrial scale.

3.1.3. Hydrogen–bromine flow battery - HBFB

A hydrogen-bromine (H_2–Br_2) flow battery mainly consists of a stack and two tanks, as a VRFB. Its electrochemical reactions are [63]:

$$\begin{aligned} &positive\ electrode: Br_2 + 2e^- \underset{charge}{\overset{discharge}{\rightleftharpoons}} 2Br^- \quad E_{0+} = +1.09\ V\ vs.\ SHE \\ &negative\ electrode: H_{2(g)} \underset{charge}{\overset{discharge}{\rightleftharpoons}} 2H^+ + 2e^- \quad E_{0-} = 0\ V\ vs.\ SHE \end{aligned} \tag{7}$$

The standard cell voltage is $E_0 = 1.09$ V. A noble metal catalyst, e.g. platinum, is needed to promote the hydrogen reactions [64]. Since bromine compounds present low activation losses, the reaction kinetics is fast, allowing high-power densities, e.g. the 1.4 W cm^{-2} measured in a 10 cm^2 single cell by Cho et al. [65]. The HFBF technology presents high volumetric energy density (>200 Wh L^{-1}) because of the high volumetric charge storage capacity of the positive electrolyte, and claims a theoretical lifespan of 10,000 h without important degradation. In real cases, the HFBF lifespan is mainly threatened by catalyst poisoning due to adsorption of bromine and bromide species [66]. The battery temperature must be kept below the boiling point of the bromine (58 °C). Bromine is abundant and cheap [66], but is also a corrosive and toxic element while hydrogen is highly flammable. Consequently, HBFBs need safety subsystems to ensure safe operation [67]. Although in a more limited extension than VRFB, HBFBs have been deployed. Among HFBFs manufactures, Elestor (Netherlands) is involved in different demonstrative projects as "Hydrous", with a 50 kW/250 kWh HBFB [68] and EnStorage (Israel) has tested a kW-class 100 kWh HBFB and detains several patents [69]. A LCOS of 0.35 € kW h^{-1} $cycle^{-1}$ has been reported [70]. Apart from hazard issues from dangerous elements, research is mainly centered on extending membrane durability, reducing bromine crossover and testing long-term performance.

3.1.4. Polyoxometalates based redox flow battery (POMs-RFB)

In the last years, the use of oxo-bridged transition-metal clusters, namely polyoxometalates, has been explored for their application in both non-aqueous and aqueous RFBs. Based on outstanding structural, electronic and reactive versatility [71,72], the main feature of those compounds is the capacity to undergo multielectron transfer reactions [73]. In turns, this leads to theoretical high volumetric capacities relying on their decent solubility, i.e. ca. 1 M in water. With a wide variety of discrete, molecular species ranging from small dimetalates to complex clusters comparable to a protein in size [74], the latter standing as the more appealing to mitigate crossover problematics common to small size metal based electrolytes. Based on the versatile structure both asymmetric and symmetric electrolytes have been developed for their use in RFBs.

POMs were first applied in aqueous media in 2013 by Anderson et al. [75]. An aqueous solution of vanadium tri-substituted Keggin-type polyoxotungstates $[XV_3W_9O_{40}]^{n-}$ (X = P, n = 9; X = Si, n = 10) [76] (20 mM) was used as symmetric electrolyte, where vanadium centers were responsible for activity of the catholyte, whereas tungsten was the redox active centre for negolyte. The tested system showed promising CE (95%), but low current density (0.5 mA cm^{-2}) and energy efficiency (<50%) due to the poor reversibility of the redox processes. A more water soluble (0.8 M) Keggin-type heteropolyacid $H_6[CoW_{12}O_{40}]$ [77] was well suited as anolyte, as tungsten-ions could store up to four electrons. The limitation of cobalt to store just one electron leads to an unbalanced volumetric capacity of 13.4 A h L^{-1} and 3.3 A h L^{-1} for the anolyte and catholyte respectively.

Cronin et al. selected the Wells-Dawson-type $[P_8W_{48}O_{62}]^{6-}$ anion as anolyte which can undergo up to 18 reduction/protonation steps in aqueous solution. Coupling with HBr/Br_2 as the catholyte counterpart results in high energy density values and nearly quantitative CE for a system cycled at 0.1 A cm^{-2} for 20 cycles [78]. A Kegging-type polyoxotungstate/polyoxovanadate $[PV_{14}O_{42}]^{9-}$ full POM RFB [79] was reported with a capacity of 10.7 A h L^{-1} for 0.1–0.2 M electrolyte, where vanadium based catholyte material shows an electron transfer rate four orders of magnitude faster than that of the VO^{2+}/VO_2^+ redox pair.

Despite the low maturity level of this technology the above-mentioned theoretical high energy density and hindered crossover in

addition to foreseen stability of POMs at different temperatures and pH values are promising aspect for the flourishing of POM based RFBs. However, there is a lack of evidence of long cycle life and the studies have only been conducted at lab-scale. This type of electrolyte has a large potential for cost reduction. Thus, the expected increase in energy storage capacity may allow to achieve an LCOS of 0.07–0.12 € $kW^{-1}h^{-1}$ $cycle^{-1}$.

3.2. Aqueous organic redox flow batteries (AORFBs)

Since most of the already mentioned problems refer to the chemistry behind the working principle of the battery, replacement of the electrolyte shows up as the most straightforward solution. In this sense, employing sustainable redox active organic molecules based on Earth-abundant elements as C, H, O, N, S; has been identified to replace commonly employed inorganic compounds. Moving forward to meet grid storage requirements will no longer pose a problem, on the contrary, those materials are expected to be inexpensively manufactured on large scale. In fact, different companies are rising based on organic materials. In Europe, Kemiwatt, Jena Batteries, Green Energy Storage and CMBlu are focused on the development of AORFBs. Kemiwatt working on quinone-based electrolyte and Jena Batteries employing pyridine-based anolyte, have successfully tested demonstrators on kW scale (20–100 kW and 400 kWh) while aiming for MW scale [80].

Besides, it has been widely accepted that the use of organic molecules as active redox materials may overcome the hurdles of VRFBs. Thus, high tunability of those compounds based on molecular engineering would allow for: i) wider cell-voltage, ii) higher solubility, iii) reduced crossover, iv) increased chemical and electrochemical stability, v) fast electrode reaction kinetics. The fact that certain organic species can lead to multiple electron transfer reactions, as well as, the possibility of employing more economical non-fluorinated membranes, serve as a proof of the high potential of those materials when aiming more cost-effective electrolytes. However, a battery that combines successfully all these parameters is still to come and generally, a compromise has to be accepted. Although high theoretical energy densities of 40–50 Wh L^{-1} and beyond could be achieved based on solubility and cell voltage, those numbers are still to be consolidated (Fig. 4a) [81,82].

A wide variety of new compounds has been investigated quinoids, quinoxalines, bipyridines, nitroxyl radicals and ferrocenes [82]. Both experimental [83,84] and computational [85–87] reports have enlightened the search for low/high potential and stable materials. However, most of them are anolyte directed efforts with limited contributions to development of new catholytes (Fig. 4b). This is one of the main reasons behind the combination of organic and organometallic or inorganic materials in what can be considered as a transition period to all-organic AORFBs. Thus, classification of materials will be done according to major groups of anolyte materials.

3.2.1. Carbonyl based electrolytes

The use of organic molecules in RFBs dates back to 2010 when Xu et al. [88] introduced BQDS (Tiron) as a water-soluble cathode material

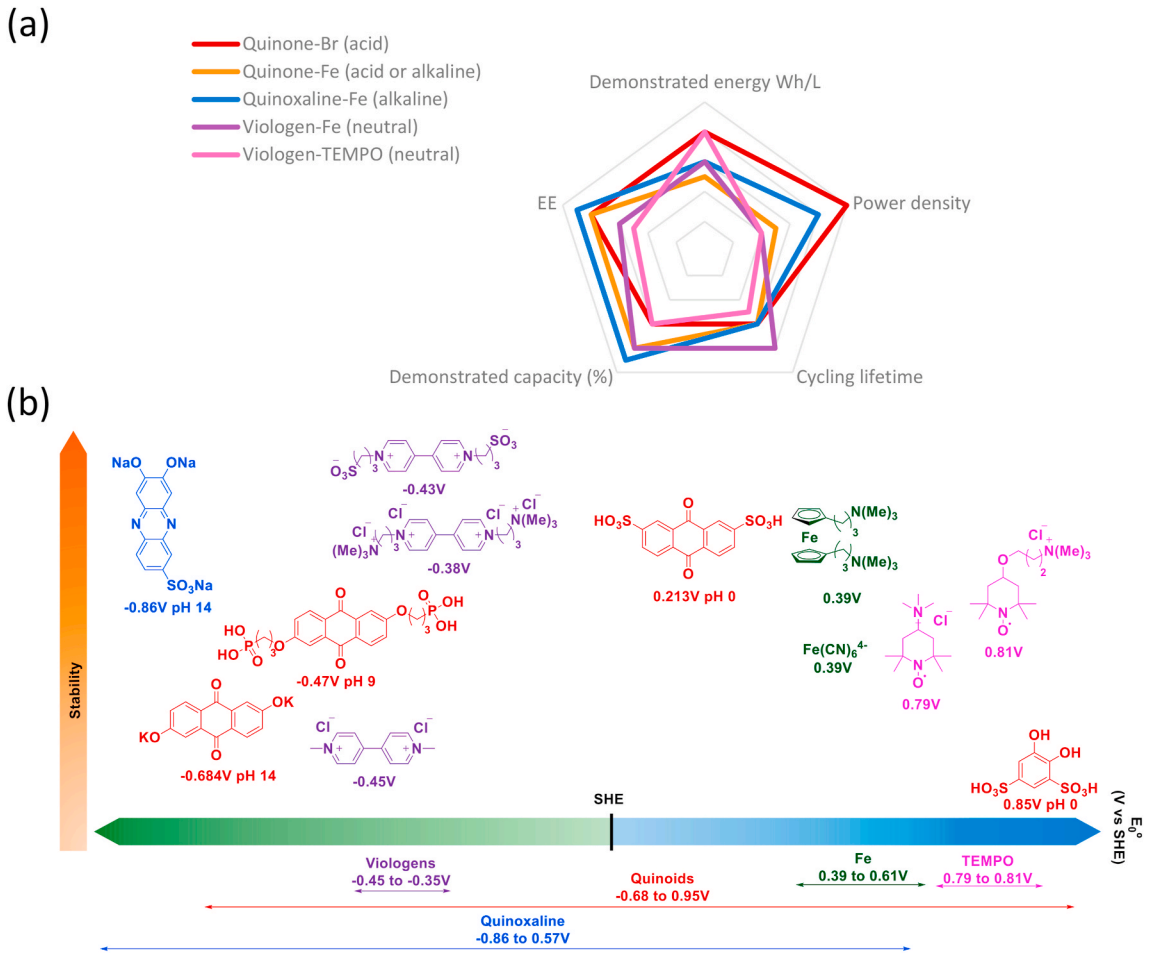

Fig. 4. (a) Reflects the compromise on key parameters and the behavior of different AORFB systems according to those. (b) Schematic overview of selected organic redox active compounds (red: benzoquinone/anthraquinone, blue: phenazine, purple: viologens, green: iron complexes, pink: TEMPO derivatives) classified according to their proven stability and redox potential recalculated to a SHE reference. (For interpretation of the references to colour in this figure legend, the reader is referred to the Web version of this article.)

in combination with $Pb/PbSO_4$ as anode. The chemistry behind this Tiron molecule is the redox equilibrium between quinone/hydroquinone couple, which is known to undergo fast $2e^-$ transfer. The use of those, so named as quinoids, has been widely explored as both anolyte and catholyte materials.

Aziz et al. introduced the use of anthraquinones as anolytes in acid media (2,7-AQDS $E_0^{\circ} = 0.213$ V vs SHE) coupled with a bromine based catholyte [89]. The AQDS/Br flow battery delivered a 0.8 V OCV and the highly conductive acid electrolyte allowed to reach excellent peak power density >0.6 W cm^{-2}. However, a high crossover rate of bromine resulted in low CE values (95%). Later on, the system efficiency was improved by membrane modification diminishing the crossover (98.35% CE) (Table 1, entry 1) [90]. 2,7-AQDS showed good stability and compatibility with bromine allowed for efficient charge/discharged for 750 cycles.

Independently Narayanan et al. [91] reported AQS/BQDS all-organic quinone AORFBs in sulfuric acid as supporting electrolyte. The use quinone/hydroquinone couple delivers low cell voltages (<0.7 V) and low capacity retention (ca. 90% for 12 cycles). In addition, the anticipated instability of Tiron [88] was confirmed as it underwent Michael type side reactions. Other related alternatives have failed to render efficient AORFBs [92,93]. Very recently, Narayanan has developed an inexpensive system based on coupling 2,7-AQDS with $FeSO_4$ (47 € kW^{-1} h^{-1}) (Table 1 entry 2) [94]. Even if this battery is clearly outperformed by already developed electrolytes pairs in some aspects as cell voltage (0.62 V), this system stands as a cost-effective candidate in terms of energy cost. Other negative aspects of the system can be listed as: the need for operating with mixed electrolyte to avoid crossover and high power related costs.

In 2015, Aziz et al. [95] adapted the quinone based system to alkaline media. The introduction of –OH groups in 2,6-DHAQ resulted in a highly soluble (>0.6 M) anolyte at pH 14 with significant decrease in the redox potential ($E_0 = -0.684$ V vs SHE). When paired with hexacyanoferrate an OCV of 1.2 V at SoC 50%, 84% EE at 100 mA cm^{-2} and 0.45 W cm^{-2} power density were reported. However, 2,6-DHAQ [96] has been identified as unstable compounds under these conditions. In fact, quinones are more prone to form reactive anion radicals above pH 9 [91]. More stable DHAQ derivatives, 2,6-DBEAQ [97] and 2,6-DPPEAQ [98] were efficiently employed in milder pH media, 12 and 9 respectively, decreasing the degradation rate (0.001% $cycle^{-1}$) of anthraquinones (Table 1, entries 3–4). AQDS salts [99,100] and alternative AQDS derivatives [101] have recently been proposed for neutral AQ-based RFBs. Although ferrocyanide was initially suggested to be highly unstable in alkaline media [102], a recent study [103] showed that charge unbalancing due to oxygen evolution reaction was the source of the capacity fading previously observed, and ferrocyanide is indeed stable.

Capacity decay related dimerization and degradation processes, including anthrone formation, Michael addition and geminal diol formation, have been identified for the family of quinones [96,104,105]. AQDS is the best candidate based on raw material cost (1–4 € kg^{-1}), while systems close to neutral pH seem to be the more stable and enable replacement of Nafion for more economical membranes (<25 € m^{-2}) [97,98].

3.2.2. Quinoxaline based electrolytes

Inspired by redox mediators as phenazine and flavin cofactors, different structures have been proposed as anolyte [106–110] and catholytes [111] for redox flow batteries. Mainly employed as anolytes in alkaline AORFBs, present high solubility, high capacity (>90% material utilization) and outstanding stability. As in the case of quinoids the redox reaction involves a $2e^-$ transfer, which depending on the pH of the media will be coupled to a protonation/deprotonation step. Wang et al. [108] developed a DHPS/$K_4[Fe(CN)_6]$ system that delivered a 1.4 V voltage, good efficiency (>75% EE) and capacity retention (99.98% $cycle^{-1}$) over 500 cycles at 100 mA cm^{-2} (Table 1 entry 5). The high capacity achieved (67 A h L^{-1}) for a highly concentrated anolyte (1.4 M, theoretical 75 A h L^{-1}) is the most remarkable feature in comparison to other systems. Phenazines and alloxazines able to reach high power density values (0.35 W cm^{-2} at 0.58 A cm^{-2}) [106] have been systematically employed with hexacyanoferrate. Long term stability experiments are required to evaluate calendar degradation as long-cycling experiments refer to large number of cycles over a short period of time.

3.2.3. Viologen based electrolytes

Viologens, as a main difference with the abovementioned redox organic materials, are used preferentially in neutral media and there is

Table 1
Comparison of the parameters reported for various AORFBs.

Anolyte/Catholyte (M)	E_0 (V)	Energy density[a] (Wh L^{-1})	Achieved capacity[b](%)	Peak power density (mW cm^{-2})	Capacity retention/cycle (n° cycles)	EE (%) at current density -(mA cm^{-2})	Membrane	Cost (€ kW^{-1} h^{-1})[d]	Ref
2,7-AQDS/HBr/Br_2 1 M/3 M (acid pH)	0.87	25.7	69	0.6–1	99.84 (750)	76 (750)	N212	–	[90]
2,7-AQDS/$FeSO_4$ 0.33 M/0.67 M (acid pH)	0.62	5.5	70	0.134	99.999924 (500)[c]	70-75 (100)	N117	47	[94]
2,6-DBEAQ/$K_4[Fe(CN)_6]$ 0.5 M/0.3 M pH 12	1.05	6.5	85	0.24	99.9993 (250)	80 (100)	E620	44	[97]
2,6-DPPEAQ/$K_4[Fe(CN)_6]$ 0.5 M/0.4 M (pH 9)	1.0	7.7	97	0.16	99.99964 (480)	65 (100)	E620	44	[98]
DHPS/$K_4[Fe(CN)_6]$ 1.4 M/0.31 M (pH 14)	1.4	18.4	90	0.14	99.98 (500)	82 (100)	N212	–	[108]
ACA/$K_4[Fe(CN)_6]$ 0.5 M/0.4 M (pH 14)	1.2	4.6	86	0.35	99.9775 (400)	74 (100)	N212	–	[107]
BTMAP-Vi/TMAP-TEMPO 1.5 M/1.5 M (neutral pH)	1.19	22.1	Ca 90	0.099	99.985 (250)	52 (100)	AMV	–	[115]
BTMAP-Vi/BTMAP-Fc 1.3 M/ 1.3 M (neutral pH)	0.75	8.0	58	–	99.9989 (500)	–	DSV	–	[117]
BTMAP-Vi/BTMAP-Fc 0.75 M/ 1 M (neutral pH)	0.75	12.2	84	0.06	99.9943 (250)	66 (50)	DSV	–	[117]
$(SPrN)_2V/NH_4[Fe(CN)_6]$ 0.9 M/ 0.9 M (neutral pH)	0.82	9.6	78	0.072	99.9997 (1000)	63 (40)	CSO	49	[120]

[a] Theoretical energy density calculated for 1:1 anolyte:catholyte ratio under given conditions.
[b] Achieved capacity was calculated as the percentage of capacity achieved from the theoretical capacity of limiting electrolyte.
[c] Long cycling at 200 mA cm^{-2}.
[d] Cost refers to electrolyte cost.

no protonation process involve in their redox equilibrium. Thus, the redox potential does not depend on pH, on the contrary, radical species are involved as intermediates or products of the reduction reaction. TEMPO derivatives [83,112–115] and iron (II) complexes as ferrocenes [116–119] or ferrocyanide [120] have been employed as the catholyte counterpart.

Methyl viologen (MV), considered as archetypical 4,4' substituted bipyridine, was firstly applied by Wang and Liu [112] in RFBs. This compound can undergo 1 or $2e^-$ reduction processes, where the second electron transfer is defined as non-reversible. In this case, unlike the quinone/hydroquinone all-organic AORFBs, catholyte and anolyte present different chemical identity, for instance, a nitroxyl radical and a viologen respectively. TEMPO is a stable radical that can undergo fast reversible redox transformation to corresponding oxoammonium salt. Recently, Aziz and Yang [115] reported a BTMAP-Vi/TMAP-TEMPO AORFB. Molecular engineering applied in this work, has served to boost both solubility ($\geq$2 M) and stability (99.985% capacity retention $cycle^{-1}$ for over 250 cycles employing 1.5 M solution of active materials) of both electrolytes while maintaining the cell voltage (1.19 V vs SHE) (Table 1, entry 7). However, TEMPO derivative still shows significant degradation over time (0.026% h^{-1}). This system was successfully combined with low cost (calculated as ca. 9 € m^{-2}) poly(phenylene oxide) based membranes leading to good chemical compatibility and permeability values comparable to commercial AEM [121].

Higher stability was delivered by BTMAP-Vi/BTMAP-Fc system (99.994% $cycle^{-1}$ over 250 cycles and 99.996% h^{-1}) under similar conditions (1.3 M vs 1.5 M for BTAMP-Vi/TMAP-TEMPO). The cycling was extended up to 500 cycles for a lower energy density system. Low current and cell voltage are limitations of this configuration (Table 1, entries 8–9) [118].

Alternatively to the use of organic compounds at both half-cells low cost materials based catholytes have been equally explored as a more practical approach, e.g. bromine (1.51 V OCV, 0.227 W cm^{-2}) [122,123], iodine [124] and iron [120]. Based on the availability and cost of the materials (ca. 1.5 € kg^{-1}) the use of $(NH_4)_4Fe(CN)_6$ in combination with $(SPr)_2V$ and an economical cation exchange membrane stands as one of the best candidates for a smooth transition to prototype level and deployment. However, the operational voltage is relatively low (0.82 V) and the use of a common electrolyte mitigates crossover and capacity decay but increases cost for active materials (Table 1 entry 10) [120].

Good cyclability, high energy density and the benefits of a neutral pH are general remarks for viologen based RFBs. On the contrary, low current and power densities are common limitations of a system working at pH 7. Currently, efforts to reach higher capacities, have been directed to unlock the $2e^-$ storage capacity of viologens. This has been achieved for viologen with extended π-conjugation [114] or hydrophilic substituents to prevent precipitation of fully reduced form [123,125].

3.2.4. Polymer-based redox active materials in RFB (PRFB)

The strategy of using redox active polymers based electrolytes is based on the maxima of developing cost-efficient redox flow batteries. The large size of those molecules is intended to be enough to completely suppress crossover and thus maintain high CE values and mitigate any capacity fading related to this phenomenon, e.g. side reactions. Moreover, the already mentioned size of the active material allows replacing standard membranes by low-cost pore size exclusion separators. Membranes are responsible of providing the ionic conductivity between half cells and contribute significantly to the overall ASR, even more as a result of aging. Commodity polymers, such as polypropylene, or inorganic materials, as silica, employed as separators would serve to decrease the cost of the cell.

Schubert et al. were pioneer on the field when his group developed a viologen-based copolymer for the anolyte and a TEMPO-based copolymer for the catholyte [126]. Those highly water-soluble polymers have acceptable viscosity values of 5 and 17 cP respectively (at theoretical specific capacity of 10 A h L^{-1}). The poly(viologen)/poly (TEMPO-*co*-METAC) RFB delivered 74.5% of theoretical capacity at 40 mA cm^{-2}. A capacity retention of 99.76% $cycle^{-1}$ over 95 cycles was recorded. More recently, the same group reported a redox active polymer with zwitterionic nature [127]. The introduction of this group allowed to reach solubilities equal to 20 A h L^{-1} in 1 M NaCl (ca. 15 mM). The zwitterionic polymer was paired with MV as anolyte to provide 1.32 V cell voltage for a theoretical 10 A h L^{-1} capacity. The cell delivered 5.33 Wh L^{-1} at 8 mA cm^{-2} over 125 cycles corresponding to an 87.5% of the theoretical energy density. A capacity retention of 99.71% $cycle^{-1}$ and 99% CE was obtained. In this case the water crossover due to osmotic pressure previously reported [128], was compensated by adding more water on the catholyte. The use of polymeric electrolytes has to face great challenges inherent to the use of high molecular weight compounds, as the low solubility, sluggish/poor reaction kinetics and high viscosity. However, this area remains unexplored and new achievements are still to come.

Development of bifunctional molecules to enable their use in symmetric systems as both anolyte and catholyte [129–132] has been targeted by researchers. However, complex synthetic routes, lower solubility and high polarization have prevented further success of this approach. Alternatively, the use of a common electrolyte specially based on low cost inorganic materials shows up as a more feasible strategy.

A deeper study of the electrolyte, including use of additives [107,133,134] or alternative counterions [120], as well as development of new electrode formulations [122] may enlarge the number of candidates to be employed as active materials. Advances in low cost-low resistance membranes are required as this component is still the main contributor to the cell ASR (ca 70%) [135]. On the other hand, outstanding anolyte materials, as DHQS, have been developed and new advances for the catholyte are required for the development of a new generation of batteries working in either acid, neutral or alkaline media. A systematic study using a variety of spectroscopic and computational means [136,137]. is expected to allow for continuous learning and problem resolution on degradation mechanism.

Currently, cost-efficient AORFBs rely on the use of low-cost iron based catholytes to meet cost targets defined by EU. Viability of AORFB will be highly dependent on active material's cost, aiming, in some cases, for $<$ 1–2 € kg^{-1}, and high stability. Recent reports [81,138] have dug into the foreseen low price of organics at large scale production and have shed light on the viability of AORFB, which may meet 0.05 € $kW^{-1}h^{-1}$ $cycle^{-1}$ target.

3.3. Pure flow membraneless

Regardless of the chemical nature of the redox material, most of the above mentioned RFB examples rely on expensive and poor performing ion-selective membranes to keep positive and negative electrolytes physically separated but ionically connected. A cost analysis of a 300 kWh VRFB showed that the electrolyte and the membrane represent ~62% and about 20–40% of the cost, respectively [35,139,140]. The use of low-cost size exclusion membranes or separators (e.g. PRFB) has been covered in previous sections. A more ambitious strategy to achieve cost effective RFBs relies on complete removal of the physical barrier between electrolytes. To date, there are only two strategies to eliminate membranes in RFBs, i) microfluidic batteries relying on hydrodynamic engineering to exploit the laminar flow of electrolytes and ii) biphasic batteries using immiscible redox electrolytes that are separated by thermodynamic principles [141] (Fig. 5).

3.3.1. Laminar flow

The first approach is based on the stream of electrolytes (mostly vanadium based) flowing through parallel micro-channels under laminar flux, which minimizes electrolyte mixing [142–149] under the adequate fluidodynamic conditions. In these microdevices, power density, which ranges from 40 mW cm^{-2} employing flow-by electrodes [143] to up to 750 mW cm^{-2} for optimized flow-through electrodes

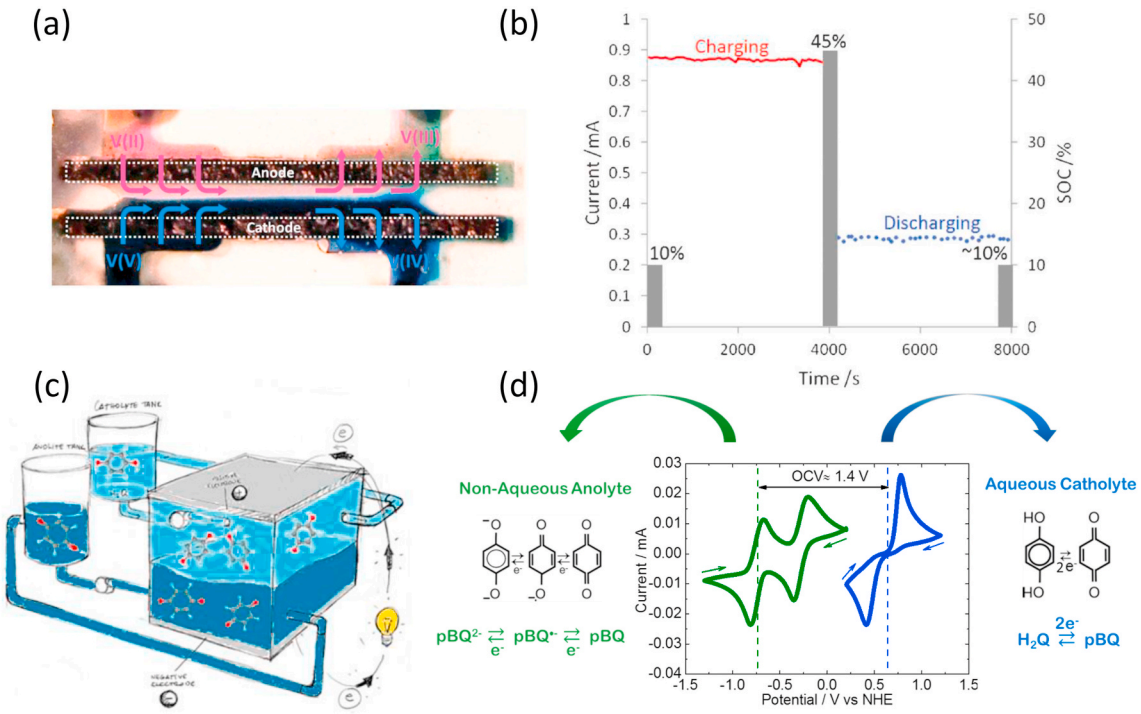

Fig. 5. a), b) Image of a microfluidic RFB and proof-of-concept operation in a complete charge-discharge cycle (Reproduced with permission from Ref. [148]) c), d) scheme of membrane-free RFB and electrochemical performance of immiscible electrolytes (Reproduced with permission from Refs. [155]).

[147], is mainly limited by the low flow rates that are necessary to maintain the laminar flow and reduce the electrolyte mixing. In fact, reactant crossover/cross-contamination and self-discharge, always present in these co-laminar microbatteries, are responsible for the low columbic efficiencies (<40%) and low reactant conversion (<20%) that limit the practical use of this technology [146]. Experimental and simulation contributions in microfluidic fuel cells have demonstrated certain mitigation of diffusive mixing while enhancing active species transport to the electrode by modifying the cell architecture, e.g. by using H-shape cross-sectional [150] or bridge-shape cross-sectional microchannels [151] or by designing optimized herringbone-inspired microstructures [152,153]. However, in all those cases the fabrication complexity increases significantly whereas crossover issue is not significantly reduced. It is important to mention that only few of those reported microfluidic electrochemical devices have been designed with a dual pass [147,148,154] instead of single pass [144] architecture making possible further electrolyte recirculation and thus battery recharging that, however, has not been demonstrated to date. Moreover, all these examples have been developed at the microscale providing much smaller power densities than their membrane-based counterparts. With single cell power output in the 10 mW range, the targeted application for co-laminar cells will be quite different from the high power conventional VRFBs with a typical 14-cell stack producing on the order of 1 kW. Therefore, their scalability is limited by the compulsory microfluidic design which restricts their practical applications to a series of commodities and small power utilities.

3.3.2. *Immiscible electrolytes*

A novel concept of Membrane-Free Battery that is not constrained to microscale design principles but based on the immiscibility of redox electrolytes has been recently explored. In the first proof-of-concept membrane-free battery reported by Navalpotro et al. [155], the biphasic system was formed by one acidic solution and one ionic liquid, both containing quinoid species. This pioneering battery which was tested in static mode exhibited an open circuit voltage of 1.4 V, a stable discharge plateau at 0.9 V and a power density of 1.98 mW cm^{-2}, being able to operate during several cycles. The versatility of this concept was demonstrated by using different aqueous-nonaqueous immiscible electrolytes (neutral aqueous, butanone, propylene carbonate, etc.) and different redox organic molecules (anthraquinones, TEMPOs) [156]. Batteries with substituted anthraquinones in the anolyte exhibited improved open-circuit voltage as high as 2.1 V with an operating voltage of 1.8 V (2 times higher) and 35% superior power density, compared to previously reported proof-of-concept. A similar approach was proposed by Bamgbopa et al. [157], who used an iron acetylacetonate complex in a hydrophobic ionic liquid phase as the negative electrolyte and iron sulfate in aqueous K_2SO_4 solution as the positive electrolyte.

The versatility of this concept has been recently expanded to aqueous-aqueous immiscible systems constituting more sustainable, more environmentally friendly, less toxic and less expensive battery chemistry [158,159]. In these cases, the aqueous biphasic systems (ABS) were formed from a ternary mixture of water and two phase-forming components such as different ionic liquids/Na_2SO_4 [158] and poly (ethylene glycol)/Na_2SO_4 [159]. Different from conventional RFB, where crossover is governed by the effectiveness of the ion-selective membrane, in these membrane-free batteries the crossover is determined by thermodynamics, specifically by the partition coefficients of active species. Methyl viologen and TEMPO were selected as the negative and positive redox species on account to their appropriate partition coefficient and redox potential. This Total Aqueous Membrane-Free Battery exhibited an OCV of 1.23 V, peak power density of 23 mW cm^{-2}, much higher than the nonaqueous-aqueous immiscible battery, and excellent long-cycling performance under static conditions. Although the crossover or cross-contamination can be suppressed by choosing species with adequate partitioning, the self-discharge at the interface is inherent to this technology and constitutes one of the most important challenges. Another important challenge is the operation of the battery under flowing conditions since commonly used filter press reactors are not appropriate here. Therefore, alternative reactor designs should be developed in near future to demonstrate if this membrane-free approach might become a real alternative.

3.4. Redox flow batteries based on insoluble solid active materials

Energy density of a conventionally designed RFB scales with solubility of the electroactive species employed, which is typically in the range of 1–2 M. On the other hand, the concentration of active centers in solid materials varies between 20 and 50 M. As a consequence, the energy density of "static" batteries based on solid active materials (e.g. Nickel–Metal Hydrides) largely surpasses the values achieved for RFBs. Instead of searching for a gradual increment in energy density by increasing the solubility, the use of solid active materials in a flowing system opens up the possibility of achieving unprecedented values for RFBs. In other words, battery technologies resulting from combining a flowing configuration and solid active materials shall possess two *incompatible* battery features, i.e. decoupled energy and power scalability and high energy density. Two main approaches (Fig. 6) have been proposed to realize this desired combination: a) the Semi-Solid Flow Battery and b) the Solid Targeted/Mediated/Boosted Flow Battery. With some exceptions, the former and the latter approaches have been focused on non-aqueous and aqueous electrolytes, respectively.

3.4.1. Semi-Solid Flow Batteries (SSFBs)

Electrolyte containing soluble active species is replaced by a suspension of solid particles that forms a slurry or also called a semi-solid electrode. The solid-containing slurry is stored in an external reservoir and pumped into the electrochemical reactor for energy conversion (Fig. 6a). The first proof-of-concept for this battery technology was demonstrated by Chiang et al. [162] using Li intercalating materials and non-aqueous electrolyte. Working prototypes of SSFBs using flowable suspensions having up to ≈12 M concentration were shown. This concept was extended to other battery chemistries based on non-aqueous electrolytes [160,163,164] and aqueous electrolytes [165–167], as well as organic particulate materials [168] and capacitive materials [169]. The main limitation regarding the use of solid active materials developed for static batteries is the new role of the solid electrolyte interphase (SEI), which turns from being a blessing in static batteries to a curse in SSFBs [170]. The SEI severs electrical connection between current collector and solid active particles so that the use of materials operating below 0.7 V vs Li/Li^+ becomes very challenging.

The use of suspensions of solid particles requires changes in the system architecture of a conventional RFBs. In particular, the reactor design should allow solid particles to flow through it. High surface area porous 3-D carbonaceous electrodes must be avoided due to the risk of clogging by the suspended particles. A typical cell reactor for SSFB is composed of two current collectors, a separator and gaskets. A space, through which a slurry will flow, is defined by gaskets [162]. The maximum current density for "flat" 2-D electrodes is drastically reduced due to the low electrochemical surface area. Carbon particles are added into the suspension of active particles to provide the slurry with electrical conductivity and thus increase the electrochemical surface area when the slurry flows through the reactor. The higher carbon content, the higher electrical conductivity and the higher current density. Unfortunately, i) the current density is still much lower than that achieved in conventional RFB configuration and ii) the viscosity and ionic resistance increase with increasing content of carbon as well, so that a compromise value of carbon content must be found. The use of surfactants, e.g. Triton X-100 and polyvinylpyrrolidone (PVP), as dispersing agents in the semi-solid electrodes was shown to improve the properties of semi-solid electrodes since this type of additive increases flowability enabling further increase in carbon content [171,172].

3.4.2. Solid Targeted/mediated/Boosted Flow batteries (SMFBs)

The use of a conventional RFB architecture is only possible when the solid active materials are confined in the external reservoirs to boost energy density (Fig. 6b). In this case, the question is how to store charges in a solid material which is centimeters or even meters away from the electrode. The answer is to use the dissolved redox species as charge carriers (redox mediator) between electrochemical reactor and external reservoir. Thus, dissolved species do not act as energy-storing materials but as molecular wiring, which allows for a drastic reduction in their concentrations. This strategy has been successfully demonstrated for several battery chemistries using a conventional RFB architecture, in which solid active materials were simply added and confined in the external reservoir, e.g. non-aqueous [173–175], aqueous acid [176], aqueous neutral [177–179] and aqueous alkaline [161] electrolytes.

The key process of this approach is the reversible and spontaneous charge transfer reaction between redox electrolyte and solid active material confined in the reservoir. When two dissolved redox species A and B with redox potentials above and below the redox potential of a solid material are used in one reservoir, species A would act as redox mediator during the charging process while species B would mediate during discharging. The main downside of using two redox mediators for each reservoir is the penalty in voltage efficiency [173]. Instead, one single redox mediator (e.g. potassium ferrocyanide) for each reservoir may be used taking advantage of the changes in redox potential of the electrolyte with the state of charge according to Nernst equation [161,179,180], solving the issue of the voltage efficiency. Perfect matching of redox potentials of redox mediator and solid active material is of critical importance for using single redox mediator. Once achieved, the solid

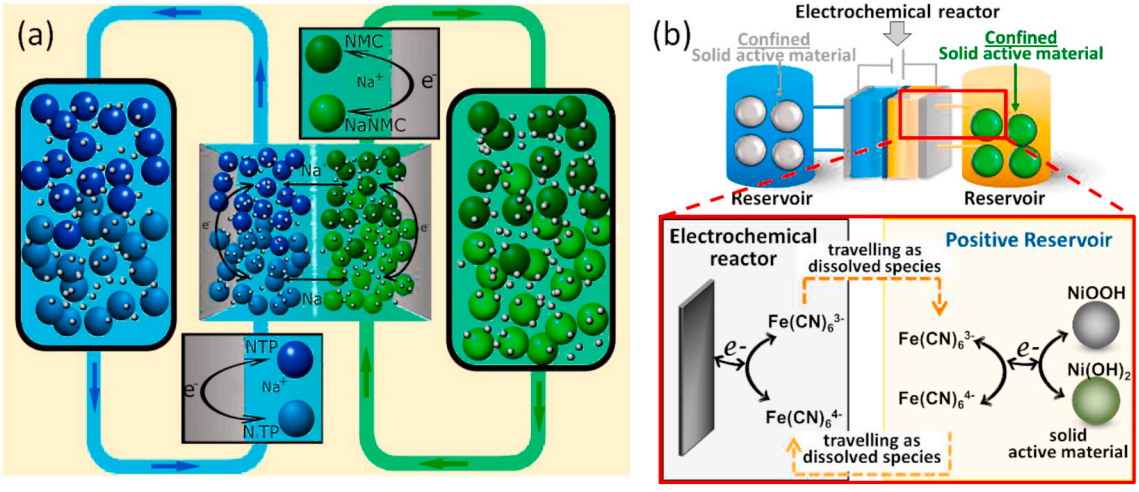

Fig. 6. Schematic representation of a) the Semi-Solid Flow Batteries and b) the Solid Targeted/Mediated/Boosted Flow batteries adapted with permission from Refs. [160,161].

active material becomes the main contributor in terms of energy density and energy cost.

3.4.3. Performance figures of RFBs based on solid active materials for aqueous electrolytes

Both SSFBs and SMFBs can potentially deliver energy densities above the-state-of-the-art values for RFBs. This feature makes both technologies especially appealing for stationary energy storage in confined spaces. Values well above 50 Wh L^{-1} for aqueous systems are accessible. For SSFB, important aspects such as shunt currents, pumping consumptions, maximum current densities (solid particles block current lines and increase ionic resistance) still require further study. Although it is certainly early to make a final assessment, energy efficiency is not expected to exceed the state-of-the-art values for RFBs. For SMFBs using a single redox mediator, the drastic decrease in the concentration of dissolved species can potentially lead to an enhancement in energy efficiency with respect to the state-of-the-art for RFBs due to the reduced energy consumption in cooling and pumping.

For SSFB, lifespan is probably the main concern due to potential mechanical degradation resulting from the continuous flow of suspended particles. This point still needs to be investigated at relevant TRLs. For SMFB, the cycle life of solid active materials will likely determine lifespan of the systems. Prussian Blue analog has demonstrated 40,000 cycles in aqueous media [181], which could result in a lifespan of above 20 years when operated at 0.3 C. However, efforts must be devoted to evaluating the actual lifespan of solid materials implemented in SMFBs to provide a reliable answer.

In SSFBs, power cost can be potentially reduced since expensive ion-selective membrane are not needed. However, operating current density must be critically evaluated since the use of suspensions increases both electrical and ionic resistances, compared to the standard RFB configuration. Nevertheless, even at 20 mA cm^{-2} for SSFB versus 100 mA cm^{-2} for conventional RFB, the power cost is reduced to the half (150 versus 300 € per kW for SSFB and conventional RFB, respectively) [166]. Further work in reactor design is recommended to minimize the thickness of flowing semi-solid electrodes, whereas pumping consumption does not increase drastically. In SMFBs, conventional RFB architecture is used so that its price will evolve with the state-of-the-art RFB. In the case of both SSFBs and SMFBs, energy cost will be dictated by the price of solid active materials. There is potential room for decreasing energy costs when materials based on abundant elements are used. For instance, the cost of Prussian Blue analogs in aqueous static batteries has been estimated to be 100 € $kW^{-1}h^{-1}$ [182]. Considering a cycle life of 40,000 cycles [181], the resulting values of 0.0025 € $kW^{-1}h^{-1}$ $cycle^{-1}$ makes plausible to achieve the cost target of 0.05 € $kW^{-1}h^{-1}$ $cycle^{-1}$ at system level set by the European Commission for 2030.

4. Alternatives for hybrid flow/non-flow batteries

ZBFBs is the most representative technology for hybrid RFBs, offering great advantages in terms of energy density. However, reported high theoretical energy density values have not been demonstrated yet and present in general low current densities. Moreover, since the bromide suffers from safety issues, alternative electrolyte formulation has been the focus of recent research. Herein, two technologies are categorized according with the cathode reaction: 1) Metal-anode in combination with solution-based redox pairs-cathode and 2) Metal-anode in combination with air (gas) cathode electrode.

4.1. Metal-solution based redox pairs flow batteries

A low-cost metal, including Zn, Fe, Cu, or Pb, is generally chosen as anode, which carries on the liquid/solid transformation. Zn, Fe and Cu are preferred based on their multiple advantages as abundant, easily recyclable and eco-friendly metals while several electrolyte solutions have been proposed for the cathode compartment. Despite these advantages, the main drawbacks of this technology are the occurrence of side-reactions, i.e. hydrogen evolution reaction (HER) and dendrite formation.

4.1.1. Zn based flow batteries

Among various suitable metals zinc excels due to its negative electrode potential in aqueous media (equation (8)) high solubility of Zn(II) ions, large volumetric capacity (5.85 A h cm^{-3}), fast electrode reaction kinetics as well as the low cost [38].

Electrochemical reactions of zinc in acid and alkaline electrolytes are as follows:

$$\begin{aligned} &\textit{Negative electrode} \quad Zn^0 \underset{charge}{\overset{discharge}{\rightleftharpoons}} Zn^{2+} + 2e^- \qquad E_{0-} = -0.76\ V\ vs.\ SHE \\ &\textit{Negative electrode} \quad Zn^0 + 4OH^- \underset{charge}{\overset{discharge}{\rightleftharpoons}} \left[Zn(OH)_4\right]^{2-} + 2e^- \quad E_{0-} = -1.25\ V\ vs.\ SHE \end{aligned} \tag{8}$$

On the other hand, zinc-based systems are typically less durable due to problems associated with uneven metal deposition during the battery charging, especially under mass transport limited conditions as a consequence of non-uniform concentration gradients [183]. The morphology of the zinc deposits is known to depend on applied charging current density and hydrodynamic conditions by the electrode [184]. The long-term operation under limiting current conditions results in harmful dendritic deposits eventually leading to battery failure due to penetration of separator by dendrites and short-circuit of the cell. The homogeneity of the deposited layer can be improved by optimized operational regime and use of organic or inorganic electrolyte additives (brighteners, levelers, etc.) [185]. Other challenges are related to HER, decreasing the efficiency and safety of the battery operation. Hydrogen can be evolved in two ways: during charging as a parasitic reaction to zinc deposition and under OCV and discharging conditions as a product of zinc corrosion, especially in acidic electrolytes [186]. Generally, lower power densities are typically reported due to limited deposition rate on planar substrates; however process can be intensified by using three-dimensional substrates (e.g., foams, felts and fabrics) [187].

Various hybrid flow batteries with the zinc based negative electrode have been developed which was recently comprehensively reviewed [38,39,188]. The key parameters of individual Zn-based flow batteries are compared in Table 2. In the following text, the main representatives of Zn-based hybrid FB are described in detail except for Zn–Br and Zn-air systems which are described in sections 2 and 4.2, respectively.

Combination of zinc negative flow half-cell with positive nickel-based half-cell (equation (9)) results in a flow battery with a high

Table 2
Comparison of the parameters reported for various zinc-based flow battery systems.

Positive half-cell element	E_0 (V)	Energy density (Wh L^{-1})[a]	Current density (mA cm^{-2})	Energy efficiency (%)	Lifetime (n° cycles)	Cost (€ kW^{-1} h^{-1})[b]	Ref.
Nickel (NiOOH)	1.73	20	80	>80	>1000	356	[189]
Iron-alkaline $K_3[Fe(CN)_6]$	1.61	34	100	86	200	79	[190]
Iron–acidic ($FeCl_3$)	1.53	25	25	<70	100	<100	[191,192]
Cerium (Ce^{4+})	2.37	25–35	50	<60	<50	N. A.	[193]
Iodine (I_3^-)	1.27	125	10	76	40	N. A.	[194]
TEMPOL (organic)	1.46	<10	10	80.4	100	N. A.	[195]

[a] Practically achieved energy density under given conditions.
[b] Cost refers to system cost.

theoretical cell voltage of 1.73 V, the so-called Zn–Ni flow (assisted) battery.

$$Positive\ electrode\quad 2NiOOH + H_2O + 2e^- \underset{charge}{\overset{discharge}{\rightleftharpoons}} 2Ni(OH)_2 + 2OH^-\quad E_{0+} = +0.49\ V\ vs.\ SHE \tag{9}$$

Although first Zn–Ni cell in static configuration was invented back in 1901 by T. Edison, the development of flow battery based on Zn–Ni chemistry started in 2007 [196]. The electrolyte flow was found efficient in suppressing shape changes of electrodes and dendrite growth when compared to static arrangement leading to increased cyclability.

As only solid-state transition takes place on positive electrode, undivided cell can be used with no membrane/separators using single electrolyte flow assisted arrangement. Short circuit of electrodes is prevented by sufficient inter-electrode distance (>4 mm) [197]. Zinc can be electrodeposited from alkaline electrolyte containing zincates on various current collectors material (Cd, Cu, Bi, Sn, Sb) with good corrosion stability and high overvoltage for HER [198]. Adaptation of three-dimensional nickel foam current collectors for negative electrode enabled efficient operation at increased current density (80 mA cm^{-2}) [187]. Sintered or pasted porous nickel hydroxide is typically used as positive electrode. Periodic reconditioning procedures using deep discharge are required for long-term stability due to zinc accumulation of negative electrode which is caused by higher coulombic efficiency of zincate reduction when compared to nickel oxidation [197]. The technology was successfully up-scaled to 25 kWh battery and tested over 1000 charge-discharge cycles with round trip energy efficiency above 80%. The cost estimates show 356 € $kW^{-1}h^{-1}$ [189].

Combination of zinc with iron based positive electrode (Zn–Fe flow battery) was developed by Lockheed Missiles and Space Company [199] in the late 1980s. Alkaline zinc-ferrocyanide flow battery provides theoretical cell voltage of 1.61 V (equation (10)) and low cost due to usage of earth-abundant elements. The technology is currently commercialized by ViZn [200] for different applications up to 1.4 MW/4.2 MWh scale [201].

$$Positive\ electrode\quad Fe(CN)_6^{3-} + e^- \underset{charge}{\overset{discharge}{\rightleftharpoons}} Fe(CN)_6^{4-}\quad E_{0+} = +0.36V\ vs.\ SHE \tag{10}$$

Negative electrode typically consists of cadmium or silver-coated substrate and a nickel-plated graphite felt is used as the positive electrode material. A cross-over of ferricyanide into the negative electrolyte is limited by divided cell using separator/membrane [38]. Recently, application of carbon felt electrodes and mechanically stable polybenzimidazole membrane significantly improved the cell performance leading to 82.8% energy efficiency (EE) at 160 mA cm^{-2}. Capital cost for such kW stack is under 80 € $kW^{-1}h^{-1}$ [190].

Apart from alkaline systems, also acidic system has been recently published, combining zinc negative electrode with positive half-cell reaction:

$$Positive\ electrode\quad Fe^{3+} + e^- \underset{charge}{\overset{discharge}{\rightleftharpoons}} Fe^{2+}\quad E_{0+} = +0.77\ V\ vs.\ SHE \tag{11}$$

Various electrolyte formulations have been suggested including acetic acid/acetate buffer [191], mixed chloride [192] and acid-alkaline pH different electrolytes [202].

High cell voltages have been reached when pairing zinc with lead (2.12 V) or cerium (2.37 V) solutions as cathode materials. Zinc-lead flow battery uses acidic sulfuric acid-based electrolyte, typically in a single-electrolyte concept, and is restricted by limited solubility of lead and zinc corrosion [190,203].

The acidic zinc-cerium flow battery, which has been developed by Plurion Inc. [193], provides high theoretical cell voltage as reflected by cerium half-cell reaction:

$$Positive\ electrode\quad Ce^{4+} + e^- \underset{charge}{\overset{discharge}{\rightleftharpoons}} Ce^{3+}\quad E_{0+} = +1.61\ V\ vs.\ SHE \tag{12}$$

Due to electrochemical instability of carbon-based materials under high potentials and low pH conditions, a noble metal, typically, platinized titanium mesh is used for positive electrode [204]. Both half-cells are mutually separated by cation-exchange PFSA membrane, however also undivided cell has been reported using a single electrolyte containing both Zn and Ce ions. The mixed acid electrolyte with an optimized ratio of sulfuric acid and methanesulfonic acid supporting electrolytes was developed to achieve sufficient solubility of Ce in both oxidation states and low rate of zinc corrosion [193].

Recently, many other zinc-based FBs have been reported. Near neutral divided cell combining zinc negative electrode with triiodide/iodide positive half-cell provides OCV of 1.26 V and high energy density up to 167 Wh L^{-1}, however low current densities have to be applied (5–10 mA cm^{-2}) [194]. The energy content can be further increased over 200 Wh L^{-1} by the addition of bromide ions serving as sequestering agents for I_2 stabilization [205]. A combination of Zn-based negative

electrode with organic redox active positive half-cell, such as 2,2,6,6-tetramethylpiperidinyl-N-oxyl (TEMPO) either monomer [195] or in the polymeric form [206,207], represent another actual trend in development of zinc-based systems.

4.1.2. Fe based flow batteries

This electrochemistry was proposed by Hruska and Savinell in 1981 [208], taking advantage of the three-valence states of the iron in order to prevent the irreversible loss of the reactant caused by crossover effect. This redox battery follows the reactions (13), and such as hybrid systems, the Fe^0 is plated/stripped in the negative compartment whilst the Fe^{2+}/Fe^{3+} couple in solution is oxidized/reduced at the carbon electrode.

$$\begin{aligned} &\textit{Positive electrode} \quad 2Fe^{3+} + 2e^- \underset{charge}{\overset{discharge}{\rightleftharpoons}} 2Fe^{2+} \quad E_{0+} = +0.77\,V\ vs.\ SHE \\ &\textit{Negative electrode} \quad Fe^0 \underset{charge}{\overset{discharge}{\rightleftharpoons}} Fe^{2+} + 2e^- \quad E_{0-} = -0.44\,V\ vs.\ SHE \end{aligned} \tag{13}$$

Furthermore, iron is an abundant material, inexpensive (electrolyte is estimated around 3% of the total cost [209]), non-toxic metal, leading to voltage cell of 1.26 V at 50% of SoC. However, the electrochemistry is pH-sensitive since the HER occurs, promoting the precipitation of Fe^{2+}. The electrolyte used was chlorine salt with high concentration of iron in NH_4Cl, providing a theoretical energy density values of 76 Wh L^{-1} (0.5 kg L^{-1} $FeCl_2$). Using microporous separator and 2 M $FeCl_2$ in 2.8 M NH_4Cl at 60 °C, energy efficiencies of 50% at 60 mA cm^{-2} and discharge peak power density of 50 mW cm^{-2} were achieved as preliminary results. However, daily pH maintenance in the anolyte is needed to keep acid environment. The ideal pH anolyte allowing the suppression of HER was 2–3, which is challenging for the positive electrolyte leading to the precipitation of $Fe(OH)_3$ in pH higher than 2. In order to improve the performance, several authors have been working to overcome this solubility issues through complexing ligands for Fe^{2+}/Fe^{3+} electrolytes. Hawthorne et al. (2014) [210] demonstrated excellent solubilities of Iron-Glycine complex ($E_0 = 468$ mV vs Ag/AgCl) in the ratio 1:1 up to pH = 2. This formulation shows a promising performance for positive electrolyte. Additionally, Tucker et al. demonstrated the low-cost chemistry for off-grid portable applications using 0.5 M $Fe_2(SO_4)_3$ in 1.2 M NaCl, delivering an energy density values of 11.5 Wh L^{-1} and power density of 20 mW cm^{-2}. The authors claim that the consumables cost for materials is below 6 € kW^{-1} h^{-1} [211].

The manufacture of all-iron redox flow battery has realized at commercial level by Energy Storage Systems Company (ESSC) and Energy Fuel®. ESSC has scaled up and commercialized all-iron redox flow battery, launching a 50 kW/400 kWh prototype with a large lifespan over more than 20,000 cycles with peak power values in the range of 33 kW–100 kW. Finally, Energy Fuel® has demonstrated this technology at 10 kW pilot plant (2016) and 100 kW field demonstration (2017), allowing the commercialization at MW level towards 2020 [212]. GRIDS programme ARPA-E targeting 110 € kW^{-1} h^{-1} system cost [213].

4.1.3. Cu based flow batteries

All-copper-hybrid redox flow battery technology could be a competitive energy storage device, providing a low cost, easily scale up, efficient and safe system for the future energy markets. Additionally, copper is an abundant material (produced in around 20 million tonnes/year), with easily recycle process and extremely lower cost (6.5 € kg^{-1}, 53 € kW^{-1} h^{-1} electrolyte cost [214]) in comparison with vanadium technology (20 € kg^{-1}). All-copper RFB exploits the three redox states of copper, following equation (14), where the Cu^+ and Cu^{2+} are species in solution and Cu^0 is platted/stripped in the electrode.

$$\begin{aligned} &\textit{Positive electrode} \quad Cu^{2+} + e^- \underset{charge}{\overset{discharge}{\rightleftharpoons}} Cu^+ \quad E_{0+} = -0.15\,V\ vs.\ SHE \\ &\textit{Negative electrode} \quad Cu^0 \underset{charge}{\overset{discharge}{\rightleftharpoons}} Cu^+ + e^- \quad E_{0-} = +0.52\,V\ vs.\ SHE \end{aligned} \tag{14}$$

The main drawback of the system is the relatively low cell voltage (~0.6 V) at fully charged state, significantly lower than other systems (>1.2 V). The proof of concept was demonstrated by Lloyd and Sanz et al. (2014) with concentrated copper solution up to 3 M in aqueous chlorine electrolytes in order to compensate the low voltage cell [215,216]. The preliminary results were quite promising, allowing excellent energy density value (ca. 20 Wh L^{-1}) which is comparable with vanadium technology. However, the operational current intensity was relatively low (20 mA cm^{-2}) as well as the energy and voltage efficiencies around 50% and 60%, respectively, operating at 40 °C. After that, several efforts have been made in order to increase this attractive technology [215]. For instance, Lloyd et al. (2015) demonstrated that the increment of the current density up to 70 mA cm^{-2} could deliver up to 37 mW cm^{-2} of power density value, using microporous separator which prevents the Cu^{2+} ions to crossover the membrane [214]. Moreover, Leung et al. (2016) studied the effect of substituting planar metal foils by porous electrodes for the electrodeposition of copper. Promising life span (ca. 35 cycles) with high coulombic and voltage efficiencies ca.99 and 72%, respectively, at 50 mA cm^{-2} and 50 °C could be achieved. Alternatively, the all copper hybrid redox flow battery has been demonstrated in deep eutectic solvents [217] and ionic liquids [218]. Nevertheless, the aqueous system is the most attractive since it provides large current output values and low-cost material.

4.2. Metal air flow batteries (MAFBs)

Metal-air flow batteries (MAFBs) rely on the same principles of classical metal air batteries (MABs), i.e. combining the lightest cathode material available in nature, i.e. oxygen, and a thin metal foil aiming for high energy density (5928 and 1218 Wh kg^{-1} theoretical capacity for Li-air and Zn-air respectively). Additionally, the flow cell design in MAFBs has been identified as a key point to overcome some of MABs challenges, mainly, limited oxygen diffusion into the cathode and passivation of electrodes by deposition of insoluble by-products or well-known uneven plating of metals and dendrite formation. Thus, the circulating media can equally enhance mass transfer of oxygen to the cell core, and of products and by-products out of the cell.

Among the several metals that have been applied in MABs [219–221], zinc, aluminum, and, more recently, lithium have been the main focus of the activity in MAFBs. Based on metal nature both aqueous and non-aqueous electrolyte media have been explored [222–224].

As a general feature, similar to their static counterparts, MAFBs typically consist of a metal anode, a separator soaked in the electrolyte, and an air (oxygen) cathode. At the anode, metal stripping/deposition occurs. At the cathode, the sluggish kinetics of the oxygen reduction and evolution reactions (ORR/OER) are promoted by catalysts that are supported on the electrode surface, typically a porous carbon with high surface area.

Different MFBs have been proposed that differ for the flow forms (solutions or slurries) and the cell design (single or double flow media and circulation) [223,225]. As an example, Fig. 7, shows the structures of MAFBs featuring, flowing anolyte (a), (b) and oxygen carrier catholyte (c), (d). The single flow media-single circulation approach stands as the most popular including both aqueous based zinc air flow batteries (Zn-MAFBs) and non-aqueous lithium air flow battery (Li-MAFB). The

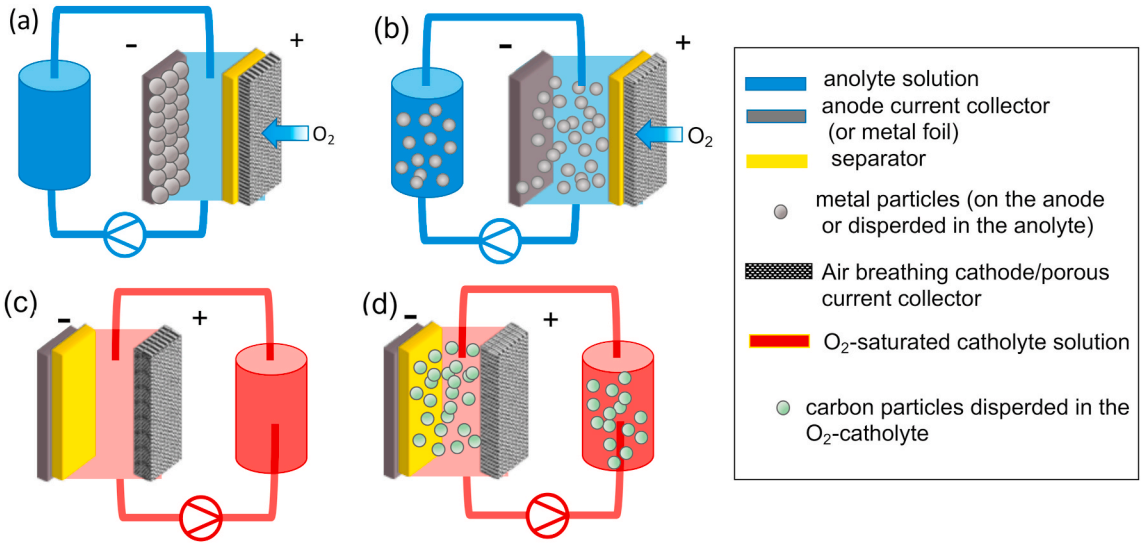

Fig. 7. Structure diagrams of MAFBs with one circulating medium. (a) Air breathing MAFB with metal anode and anolyte solution flow; (b) Air breathing MAFB with metal slurry anolyte, MAFB with metal anode and an oxygenated catholyte solution (c) or oxygenated suspension of carbon, slurry catholyte (d).

former has reached higher TRL based on safety and cost aspects.

Electrochemical reactions in Zn-MAFBs proceed as follows:

$$\begin{aligned} &\textit{Positive electrode} && O_2 + 2H_2O + 4e^- \underset{charge}{\overset{discharge}{\rightleftharpoons}} 4OH^- && E_{0+} = +0.4\ V\ vs.\ SHE \\ &\textit{Negative electrode} && Zn^0 + 4OH^- \underset{charge}{\overset{discharge}{\rightleftharpoons}} Zn(OH)_4^{2-} + 2e^- && E_{0-} = -1.25\ V\ vs.\ SHE \end{aligned} \quad (15)$$

Anolyte for Zn-MAFBs can be present either as a typical Zn^{2+} electrolyte flowing solution and a zinc metal foil located in the cell [226] (Fig. 7a), or as a slurry containing metal particles [227] (Fig. 7b). In the former case, any discharge product that might passivate the metal, i.e. ZnO is removed out of the cell core by the electrolyte circulation, with a positive effect on cell discharge capacity and cycle life. As a general remark, the electrolyte circulation mitigates both passivation and dendrite formation phenomenon.

Alternatively, the use of a metal slurry has the advantage of avoiding dendrite formation and surface passivation, metal dissolution and precipitation occur in the flowing anolyte. The cells with this configuration can be recharged mechanically, i.e. "refilled" by replacing the aged anolyte with a fresh slurry. The aged anolyte is then recovered by zinc reduction outside the cell, in a separate environment. High power densities are generally obtained with this configuration, whilst critical issues are the clog problems and finding a way to fully utilize metal particles in the slurry. Aqueous Zn-MAFB cells, with an anode composed of zinc pellet beds intercepting the KOH electrolyte flow and with an MnO_2 cathode catalyst, were capable to deliver peak power densities of 435 mW cm^{-2}. This Zn -MABF concept was also successfully upscaled at stack level. A stack of 5 cells, delivered a peak power of 138 W [227]. While cell refueling is an option, it requires that the Zn-anolyte is regenerated ex-situ, even by chemical processes. This means that by this operation, this kind of Zn-MAFBS are rather to be considered as primary cells.

At cell level, an improved electrochemical cyclability of Zn-MAFBs has been demonstrated by the use of decoupled bi-functional cathodes. A cell that exploited two positive electrodes, one for the charge process and the second one for the discharge achieved 600 charge/discharge cycles [228]. A 1 kW/4 kWh stack, comprising 20 cells connected in series, fed with a $Zn(OH)_4^{2-}$ anolyte and with decoupled, bifunctional catalysts was reported. Despite single cells exhibited good cycling performance over 2000 cycles, shunt currents dramatically lowered the coulombic efficiency of the stack to 18.3% [229]. New bifunctional catalysts are needed to elongate cyclability, to decrease overvoltage and improve the energy efficiency of Zn-MABs, that, today, is still lower than 70%.

Zinc 8 currently commercializing 100 kW Zn-MAFBs, is targeting in the next years 1 MW installation at a price that is expected to fall down below 100 € $kW^{-1}h^{-1}$ by 2023. The low cost is also dictated by the possibility of recycling Zn, that, after discharge, is regenerated in the external tanks [230]. The addressed market is stationary storage in MWh-renewable energy plants. As a reference, the cost of aqueous static Zn- is only 0.002 € $kW^{-1}h^{-1}$ $cycle^{-1}$ [224].

Despite at their infancies compared to Zn-MAFBs, non-aqueous Li-MAFBs, for their exceptionally high energy density are holding a great promise for energy storage.

The main electrode reactions in Li-MAFBs are:

$$\begin{aligned} &\textit{Positive electrode} && O_2 + 2Li^+ + 2e^- \underset{charge}{\overset{discharge}{\rightleftharpoons}} Li_2O_2 && E_{0+} \simeq 0\ V\ vs.\ SHE \\ &\textit{Negative electrode} && Li^0 \underset{charge}{\overset{discharge}{\rightleftharpoons}} Li^+ + e^- && E_{0-} = -3\ V\ vs.\ SHE \end{aligned} \quad (16)$$

In Li-MAFBs, a lithium foil anode was coupled to an organic O_2-saturated catholyte (Fig. 7c). The catholyte flow accelerates O_2 feeding rate to the cathode current collector based on porous carbon layer. It also serves to mitigate dendrite formation as well as to circulate insoluble species as Li_2O_2 to prevent electrode passivation during discharge and increase electrode-electrolyte interface during charge, therefore improving the practical discharge capacity of the cell. The use of high

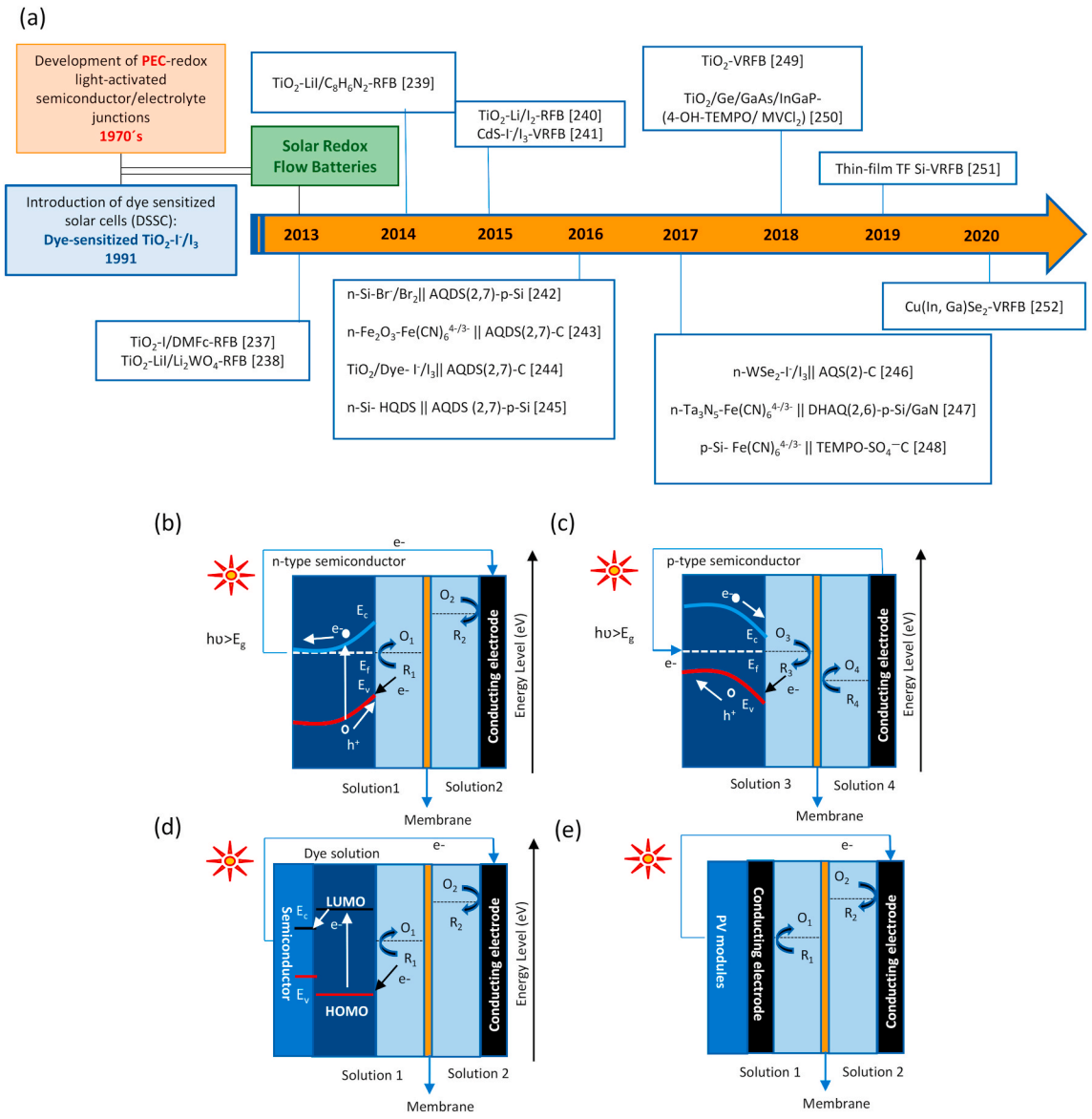

Fig. 8. (a) SRFB timeline. Photocharging mechanism under illumination for single n-type (b) and p-type semiconductor (c) in contact with the solution, dual system is a combination of (a) and (b); DSSC where solution 1 could contain I^-/I_3^- (d); and PV modules accoupled to RFB's stack (e).

reactive metals as lithium or sodium requires of ceramic separator to prevent O_2, N_2 and CO_2 crossover. A cell working with an ionic liquid based catholyte achieved a practical discharge capacity up to 600 mA h g^{-1} of carbon electrode under discharge currents of 0.2 mA cm^{-2}, with a coulombic efficiency of 92% [231,232]. Alternatively, using a semi-solid catholyte that incorporated carbon particles discharge capacity and current rate response were further improved and a practical specific energy of 500 Wh kg^{-1} was achieved whilst recharge overvoltages were decreased [233] (Fig. 7d). Specifically, a catholyte based on 0.5 mol L^{-1} of lithium bis(trifluoromethanesulfonyl)imide (LiTFSI) in tetraethylene glycol dimethyl-ether (TEGDME) with g 10 wt% Pureblack® was cycled 120 times with an areal capacity of 4 mA h cm^{-2} and currents higher than 0.5 mA cm^{-2} [234]. These promising results are under exploitation by the StartUp Bettery that is prototyping a semi-solid Li-MAFB with the challenging target cost of 130 € $kW^{-1}h^{-1}$ [235]. Other approaches of Li-MAFBs present a catholyte featured with a redox mediator that is reduced at the air electrode and regenerated in the external unit while producing Li_2O_2 that, therefore, precipitates outside of the cell and extends cyclability [236].

Low energy efficiency of Zn-MAFBs, low power density of Li-MAFBs are main challenges to be faced by those technologies in addition to the limited cyclability demonstrated in MAFBs. Little is known on the impact of the flow on the electrodes, especially on the porous carbon at the catholyte and possible changes on the morphology. Further improvements are required to improve cathode triple phase boundary to achieve a high conversion efficiency and fast cell response under high-current regimes.

5. Emerging technologies

Although high performance RFBs have been demonstrated even at market level, the research for optimized RFB technology has been appealing for Today's R&D community. In this scenario, solar rechargeable RFB batteries appear as emerging technologies to tackle the photovoltaic intermittency issues. In parallel, to achieve the industrial acceptance, new chemistries using inexpensive and unlimited materials have been implemented to gain an advantage in lifespan and energy density values. In this section, disruptive technologies are introduced as emerging RFB system.

5.1. Solar redox flow batteries (SRFBs)

The integration of photoelectron-conversion electrodes into redox flow batteries (so-called Solar redox flow batteries, SRFB) is a promising energy storage technique, offering a cost-effective way for the next-generation redox flow batteries (RFB) application in two aspects: i) Operational overpotential of the RFB is greatly reduced for the contribution of the photovoltage; ii) Efficient design, fewer packaging in a compact device for physical size-required applications. The SRFB technology has been developed since 1970 in parallel with RFB (Fig. 8a) [237–252].

The system has been engineered in two architectures, enabling several photocharging mechanism (Fig. 8b):

(1) Photo-assisted electrode: i) Photo-electrochemical (PEC), and ii) Dye sensitized solar cells (DSSC). The semiconductor-liquid junction cell is performed matching the energy-level of the semiconductor and redox couple, defining the photovoltage of the cell.
(2) Direct integration of the photovoltaic (PV) module, which is stacked together with the electrochemical module of RFB, operating autonomously. The photovoltage is generated by PV module, independently of energy levels of the redox couple and semiconductor.

Despite of the state-of-the-art progress, the SRFB technology is in an infancy R&D stage, trying to overcome several drawbacks related with the low-capacity, insufficient photovoltage, efficient, and stable materials. To date, all SRFB prototypes have been demonstrated with metal (i.e. all Vanadium) or organic molecules as well as combination of both (i.e. metal-organic molecules) as electroactive species in aqueous electrolyte. The record-breaking conversion solar-to-output electricity efficiency (SOEE) of 14.1% was achieved by Li.et al. (2018). They demonstrated the feasibility of achieving excellent photopotential (i.e. 2.4 V), using the monolithic (TiO_2/Ge/GaAs/InGaP) PV modules integrated into RFB. This RFB system operates with (0.1 M) 4-OH-TEMPO and (0.1 M) methyl viologen as the catholyte and the anolyte respectively. Under 1-sun illumination (100 mW cm^{-2}), a 14 mA cm^{-2} of photocurrent value was obtained, keeping stable over 10 cycles [250]. Motivated by these findings, Urbain et al. (2019) demonstrated, for the first time, a bias free SVRFB operating in real concentration of vanadium electrolytes (1.6 M), using triple junction TF silicon solar cell under illumination (300 mW cm^{-2}). The authors achieved 25 mA cm^{-2} as bias free-photocurrent, enabling 54 Wh L^{-1} as energy density values, while the SOEE was roughly 10% [251].

5.2. Air-breathing sulfur flow batteries

The emerging "Air-Breathing aqueous sulfur flow battery" (Li_2Sx/air or Na_2Sx/air) [253] takes advantage of using inexpensive chemicals, achieving competitive prices (being limited by precious metals used by cathode electrodes); less than 1 € $kW^{-1}h^{-1}$ using Na_2S chemicals. The battery could work in both electrolytes; acid or alkaline, giving a E^0 roughly 1.26 V at neutral pH (equations (17) and (18)).

$$\begin{aligned} &\textit{Positive electrode} \quad O_2 + 4H^+ + 4e^- \underset{charge}{\overset{discharge}{\rightleftharpoons}} 2H_2O \qquad E_{0+} = +1.29\ V\ vs.\ SHE \\ &\textit{Negative electrode} \quad xS_x^{2-} \underset{charge}{\overset{discharge}{\rightleftharpoons}} xS_y^{2-} + 2(y-x)e^- \qquad E_{0-} = -0.447\ V\ vs.\ SHE \end{aligned} \tag{17}$$

$$\begin{aligned} &\textit{Positive electrode} \quad O_2 + 2H_2O + 4e^- \underset{charge}{\overset{discharge}{\rightleftharpoons}} 4OH^- \qquad E_{0+} = +0.401\ V\ vs.\ SHE \\ &\textit{Negative electrode} \quad xS_x^{2-} \underset{charge}{\overset{discharge}{\rightleftharpoons}} xS_y^{2-} + 2(y-x)e^- \qquad E_{0-} = -0.447\ V\ vs.\ SHE \end{aligned} \tag{18}$$

The proof of the concept has been demonstrated in flow mode (10 mL min^{-1}) using dual cathode configuration based on IrO_2 (for OER) in combination with gas diffusion layer with Pt/C (for ORR) and Sulfided Ni Mesh as anode. Both compartments were separated by LISICON membrane. 1 M Li_2S_4 in 1 M LiOH serves as anolyte, while 0.5 M Li_2SO_4 + 0.5 M H_2SO_4 serves as catholyte. Cyclability studies demonstrated promising lifespan for the Li_2Sx/air RFB, achieving 49 cycles (960 h) at 0.325 mA cm^{-2} with a 55% of round-trip voltage efficiency at 55 °C. On discharge, the RFB can deliver a 3.2 mW cm^{-2} at 6.0 mA cm^{-2}. The authors state that the system is limited by the membrane resistance.

5.3. Metal-CO_2 batteries

It is well-known that CO_2 emissions is one of the world's most pressing challenges against climate change. Nowadays, the recycling of CO_2 and its conversion to value-added chemicals is a sustainable and reliable route to solve the future social problem. In this framework, CO_2 reduction coupled with the generation of electricity could represent an eco-friendly and economical solution. This idea was exploited by Wang et al. (2020), demonstrating the Zn– CO_2 flow battery concept [254]. Here, a one-compartment cell is used with a nanofiber as cathode, which is fed with CO_2 in a flow mode; and Zn wire as anode, working in a static mode. [EMIM][BF_4] ionic liquid was used as electrolyte. The working principle is the oxidation of zinc to Zn $(OH)_2$ in the anode, which provide e^-/H^+ to cathode for the CO_2-to-CH_4 conversion (Faradaic efficiency (FE) = 94%) (equation (19)).

$$\begin{aligned} &\textit{Positive electrode} \quad CO_2 + 8H^+ + 8e^- \underset{charge}{\overset{discharge}{\rightleftharpoons}} CH_4 + H_2O \quad E_{0+} = -0.24\ V\ vs.\ SHE\ at\ pH = 7 \\ &\textit{Negative electrode} \quad Zn^0 + 2OH^- - 2e^- \underset{charge}{\overset{discharge}{\rightleftharpoons}} Zn(OH)_2 \quad E_{0-} = -1.24\ V\ vs.\ SHE \end{aligned} \tag{19}$$

This new strategy could replace the traditional CO_2 electrolysers,

that involve oxygen evolution reaction, that implies a large overpotential and high cell voltage (i.e. roughly 1.5 V to produce CO). Furthermore, the authors claim that the battery generates an energy density of 288.3 Wh kg^{-1} (based on the zinc mass), as well as the feasibility to regenerate Zn metal anode *in situ* by supplying energy, which can be replaced in the future applications by renewable energy.

6. Conclusions and perspectives

Several technologies are being commercialized, VRFB, ZBFB, IRFB, HBFB, AORFB among others, where VRFB is the technology more diffused and successful. Availability and cost of vanadium to face great energy storage demand is the main limitation for VRFB. Efforts continue to improve components (i.e. electrolyte composition, membrane and electrode), performance (efficiency and power and current densities) and business approach to bridge the gap with defined targets. Substituting the problematic catholyte material as proposed in VOFB and VBFB implies a high uncertainty level for technologies still far from maturity and with identified issues as handling of toxic bromine, common to ZBFBs and HBFBs, or need for a catalyst to use of air/oxygen reactants.

A general strategy to decrease cost looks at alternative chemistries. POMs and AORFB propose highly tuneable and potentially high-performing materials although the former is at an infancy stage. The use of organics is foreseen as an option to assess the high demand for energy storage based on the availability of materials and the reduced cost deriving from large scale production. Current research efforts aim to reduce degradation rate, identified as the main shortcoming, and improve performance. Electrolytes less aggressive and/or able of limited crossover across the separator may enable a reduction of the power module cost thanks to cheaper separators. The wide range of materials available for AORFB, complemented by high-throughput screening and computational investigations, could result in the irruption of new chemistries for RFBs.

Among different approaches to hybrid RFBs, despite the early success of ZBFBs, there is a trend towards low-cost safe materials, such as Zn–Fe flow batteries that are already commercially available. Risks inherent to metal plating, e.g. dendrite formation, have hindered larger deployment. Efforts focus on increasing current density and efficiency particularly problematic for MAFBs with more complex redox processes and different phases involved. Despite operational limitations, these technologies are likely to meet cost targets as of low-cost employed materials and innovative low-cost All-iron, All-copper and zinc air batteries could hit particularly low LCOS values. More real environment demonstration results should be pursued to achieve the social acceptance. Li-MAFBs hold great promise in terms of energy density but its applicability to stationary storage in terms of safety, cost and lifespan is uncertain.

Complete removal of the physical barrier between electrolytes will imply a significant decrease in the battery cost. Microfluidic batteries rely on hydrodynamic engineering to exploit the laminar flow of electrolytes and further developments on battery architecture are needed to enable recharging. According to their microfluidic design, application of these batteries is limited to a series of commodities and small power utilities. Biphasic batteries using immiscible redox electrolytes that are separated by thermodynamic principles are a better option to be scaled-up, although still at low maturity level. Alternative reactor designs are required to consolidate the membrane-free approach. Self-discharge has been identified as the most important challenge.

The use of insoluble solid electroactive materials in redox flow batteries allows the increase of energy density. In the semi-solid flow battery (SSFB), solid materials are pumping as flowable slurries through entire systems, eliminating the need for expensive ion-selective membranes in the power conversion reactor. In the solid mediated flow battery (SMFB), solid materials are confined in the external reservoirs so that dense and viscous slurries do not need to be continuously pumped. In both cases, energy cost will be dependent on the energy cost of the solid materials. Still, much efforts need to be devoted to these immature two battery technologies to be able to foreseen their full potential.

Thus, research and development aiming low cost RFBs should focus not only on economical materials but also on the optimized system performance, mainly as regards energy density and power density, while maintaining high efficiencies. The technologies and advances outlined in this review can be combined and deeper knowledge acquired for more stablished technologies should serve as guidance for smooth promotion of recent scientific breakthroughs still at low TRLs. According to long lifetime and large scale application characterizing RFBs for stationary energy storage targets, stability and safety of the employed materials are crucial to guarantee the sustainability and to ensure the final success. Those aspects have a pivotal importance on viability and cost. In this sense, there is a continous flow of disrupting ideas such as SRFB or CO_2-based RFBs that may lead to new generation of redox flow batteries in accordance to society needs and interests. Those, at low maturity level, are under development, presenting challenges in the efficiency, stability and the energy density.

All in all, significant improvements have been achieved in the field of RFBs and future efforts will allow RFBs to continue paving the road to 2030 targets (10,000 cycles and 0.05 € $kW^{-1}h^{-1}$ $cycle^{-1}$) in view of the wider spread of sustainable electrochemical energy storage. European Commission is supporting the consecution of this research through the HORIZON2020 call LC-BAT-3 and 4 fully devoted to RFBs, e.g. innovative technologies as AORFB and All-copper RFB are supported by this initiative aiming to reach high TRLs.

CRediT authorship contribution statement

Eduardo Sánchez-Díez: Writing - original draft, Writing - review & editing. **Edgar Ventosa:** Writing - original draft, Writing - review & editing. **Massimo Guarnieri:** Writing - original draft, Writing - review & editing. **Andrea Trovò:** Writing - original draft, Writing - review & editing. **Cristina Flox:** Writing - original draft, Writing - review & editing. **Rebeca Marcilla:** Writing - original draft, Writing - review & editing. **Francesca Soavi:** Writing - original draft, Writing - review & editing. **Petr Mazur:** Writing - original draft, Writing - review & editing. **Estibaliz Aranzabe:** Writing - original draft, Writing - review & editing. **Raquel Ferret:** Writing - review & editing.

Declaration of competing interest

The authors declare that they have no known competing financial interests or personal relationships that could have appeared to influence the work reported in this paper.

Acknowledgements

This work has been supported by the European Union under HIGREEW, Affordable High-performance Green Redox Flow batteries (Grant Agreement no. 875613) and CuBER, Copper-Based Flow Batteries for energy storage renewables integration (Grant agreement no: 875605) projects. Basque Government (GV-ELKARTEK-2020 KK-2020/00078), Spanish MINECO (RTI2018-099228-A-I00 and RYC2018-026086-I (Ramon y Cajal fellowship) E.V.) and CDTI (Centro para el Desarrollo Tecnológico Industrial, CER-20191006) are also acknowledged for funding this work. R.M. thanks the European Research Council (ERC) through "MFreeB" project (grant agreement no. 726217) for financial support.

References

[1] The European Green Deal, COM, 2019, p. 640, 11.12.2019.
[2] Report on the Implementation of the Strategic Action Plan on Batteries: Building a Strategic Battery Value Chain in Europe, COM, 2019, p. 640, 176 final, 9.4.2019.

[3] The national academies summit on America's energy future: summary of a meeting, N. R. C. Committee for the National Academies Summit on America's Energy Future, National Academies Press, Washington, DC, 2008.

[4] Action 7 of the SET Plan on "Batteries for e-mobility and stationary storage. https://setis.ec.europa.eu/system/files/integrated_set-plan/action7_issues_paper.pdf.

[5] G.L. Soloveichik, Flow batteries: current status and trends, Chem. Rev. 115 (2015) 11533–11558, https://doi.org/10.1021/cr500720t.

[6] J. Noack, N. Roznyatovskaya, T. Herr, P. Fischer, The chemistry of redox-flow batteries, angew chem int ed engl 54 (2015) 9776–9809, https://doi.org/10.1002/anie.201410823.

[7] C. Zhang, L. Zhang, Y. Ding, S. Peng, X. Guo, Y. Zhao, G. He, G. Yu, Progress and prospects of next-generation redox flow batteries, Energy Stor. Mater. 15 (2018) 324–350, https://doi.org/10.1016/j.ensm.2018.06.008.

[8] J. Winsberg, T. Hagemann, T. Janoschka, M.D. Hagger, U.S. Schubert, Redox-flow batteries: from metals to organic redox-active materials, angew chem int ed engl 56 (2017) 686–711, https://doi.org/10.1002/anie.201604925.

[9] X. Ke, J.M. Prahl, J.I.D. Alexander, J.S. Wainright, T.A. Zawodzinski, R. F. Savinelli, Rechargeable redox flow batteries: flow fields, stacks and design considerations, Chem. Soc. Rev. 47 (2018) 8721–8743, https://doi.org/10.1039/C8CS00072G.

[10] P. Alotto, M. Guarnieri, F. Moro, Redox-Flow Batteries for the storage of renewable energy: a review, Ren. Sust. Energ. Rev. 29 (2014) 325–335, https://doi.org/10.1016/j.rser.2013.08.001.

[11] Vanitec Transforming Possibilities, Vanadium Redox Flow Battery Company, 2020. http://www.vanitec.org/vanadium-redox-flow-battery-vrfb-companies. (Accessed 10 September 2020).

[12] Vanitec Transforming Possibilities, Vanadium Redox Flow Battery (VRFB) technology is increasingly being tested or deployed across the globe, 2020. https://willigandital/pr/bold-editorial/vanitec/v3/. (Accessed 10 September 2020).

[13] K. Knehr, E.J.E.C. Kumbur, Open circuit voltage of vanadium redox flow batteries: discrepancy between models and experiments, Electrochem. Commun 13 (2011) 342–345, https://doi.org/10.1016/j.elecom.2011.01.020.

[14] L. Li, S. Kim, W. Wang, M. Vijayakumar, Z. Nie, B. Chen, J. Zhang, G. Xia, J. Hu, G. Graff, A stable vanadium redox-flow battery with high energy density for large-scale energy storage, Adv. Energy Mater 1 (2011) 394–400, https://doi.org/10.1002/aenm.201100008.

[15] S. Roe, C. Menictas, M. Skyllas-Kazacos, A high energy density vanadium redox flow battery with 3 M vanadium electrolyte,, J. Electrochem. Soc. 163 (2016) A5023–A5028, https://doi.org/10.1149/2.0041601jes.

[16] J. Charvát, P. Mazúr, J. Dundálek, J. Pocedič, J. Vrána, J. Mrlík, J. Kosek, S. Dinter, Performance enhancement of vanadium redox flow battery by optimized electrode compression and operational conditions, J. Energy Storage 30 (2020) 101468–101477, https://doi.org/10.1016/j.est.2020.101468.

[17] D. Aaron, Q. Liu, Z. Tang, G. Grim, A. Papandrew, A. Turhan, T. Zawodzinski, M. Mench, Dramatic performance gains in vanadium redox flow batteries through modified cell architecture, J. Power Sources 206 (2012) 450–453, https://doi.org/10.1016/j.jpowsour.2011.12.026.

[18] M. Guarnieri, A. Trovò, G. Marini, A. Sutto, P. Alotto, High current polarization tests on a 9 kW vanadium redox flow battery, J. Power Sources 431 (2019) 239–249, https://doi.org/10.1016/j.jpowsour.2019.05.035.

[19] R. Monteiro, J. Leirós, M. Boaventura, A. Mendes, Insights into all-vanadium redox flow battery: a case study on components and operational conditions, Electrochim. Acta 267 (2018) 80–93, https://doi.org/10.1016/j.electacta.2018.02.054.

[20] D. Reynard, C. Dennison, A. Battistel, H.H. Girault, Efficiency improvement of an all-vanadium redox flow battery by harvesting low-grade heat, J. Power Sources 390 (2018) 30–37, https://doi.org/10.1016/j.jpowsour.2018.03.074.

[21] D. Bryans, V. Amstutz, H.H. Girault, L.E. Berlouis, Characterisation of a 200 kW/400 kWh vanadium redox flow battery, Batteries 4 (2018) 54–69, https://doi.org/10.3390/batteries4040054.

[22] M. Guarnieri, A. Trovò, F. Picano, Enhancing the efficiency of kW-class vanadium redox flow batteries by flow factor modulation: an experimental method, Appl. Energy 262 (2020) 114532–114542, https://doi.org/10.1016/j.apenergy.2020.114532.

[23] R.L. Fares, J.P. Meyers, M.E. Webber, A dynamic model-based estimate of the value of a vanadium redox flow battery for frequency regulation in Texas, Appl, Energy 113 (2014) 189–198, https://doi.org/10.1016/j.apenergy.2013.07.025.

[24] A. Lucas, S. Chondrogiannis, Smart grid energy storage controller for frequency regulation and peak shaving, using a vanadium redox flow battery, Int. J. Elec. Power 80 (2016) 26–36, https://doi.org/10.1016/j.ijepes.2016.01.025.

[25] A. Trovò, F. Picano, M. Guarnieri, in: 2019 IEEE 28th International Symposium on Industrial Electronics (ISIE), IEEE, 2019, pp. 1977–1982.

[26] A. Trovò, F. Picano, M. Guarnieri, Comparison of energy losses in a 9 kW vanadium redox flow battery, J. Power Sources 440 (2019) 227144–2271454, https://doi.org/10.1016/j.jpowsour.2019.227144.

[27] M. Guarnieri, P. Mattavelli, G. Petrone, G. Spagnuolo, Vanadium redox flow batteries: potentials and challenges of an emerging storage technology, IEEE Ind. Electron. M 10 (2016) 20–31, https://doi.org/10.1109/MIE.2016.2611760.

[28] A. Trovò, Battery management system for industrial-scale vanadium redox flow batteries: features and operation, J. Power Sources 465 (2020) 228229–228240, https://doi.org/10.1016/j.jpowsour.2020.228229.

[29] M. Guarnieri, A. Bovo, A. Giovannelli, P. Mattavelli, A real multitechnology microgrid in venice: a design review, ieee Ind. Electron. M 12 (2018) 19–31, https://doi.org/10.1109/MIE.2018.2855735.

[30] N.V. Roznyatovskaya, V.A. Roznyatovsky, C.-C. Höhne, M. Fühl, T. Gerber, M. Küttinger, J. Noack, P. Fischer, K. Pinkwart, J. Tübke, The role of phosphate additive in stabilization of sulphuric-acid-based vanadium (V) electrolyte for all-vanadium redox-flow batteries, J. Power Sources 363 (2017) 234–243, https://doi.org/10.1016/j.jpowsour.2017.07.100.

[31] F.J. Oldenburg, T.J. Schmidt, L. Gubler, Tackling capacity fading in vanadium flow batteries with amphoteric membranes, J. Power Sources 368 (2017) 68–72, https://doi.org/10.1016/j.jpowsour.2017.09.051.

[32] N. Bevilacqua, L. Eifert, R. Banerjee, K. Köble, T. Faragó, M. Zuber, A. Bazylak, R. Zeis, Visualization of electrolyte flow in vanadium redox flow batteries using synchrotron X-ray radiography and tomography–Impact of electrolyte species and electrode compression, J. Power Sources 439 (2019) 227071–227080, https://doi.org/10.1016/j.jpowsour.2019.227071.

[33] C. Minke, U. Kunz, T. Turek, Techno-economic assessment of novel vanadium redox flow batteries with large-area cells, J. Power Sources 361 (2017) 105–114, https://doi.org/10.1016/j.jpowsour.2017.06.066.

[34] M. Moore, C. Robert, J. Watson, A. Thomas, C. Sun, An analysis of the contributions of current density and voltage efficiency to the capital costs of an all vanadium redox-flow battery, J. Chem. Eng. Process Technol. 7 (2016) 288–292, https://doi.org/10.4172/2157-7048.1000288.

[35] V. Viswanathan, A. Crawford, D. Stephenson, S. Kim, W. Wang, B. Li, G. Coffey, E. Thomsen, G. Graff, P. Balducci, Cost and performance model for redox flow batteries, J. Power Sources 247 (2014) 1040–1051, https://doi.org/10.1016/j.jpowsour.2012.12.023.

[36] S. Weber, J.F. Peters, M. Baumann, M. Weil, Life cycle assessment of a vanadium redox flow battery, Environ. Sci. Technol. 52 (2018) 10864–10873, https://doi.org/10.1021/acs.est.8b02073.

[37] Bushveld Minerals, About Bushveld Minerals, 2019. https://www.bushveldminerals.com/. (Accessed 10 September 2020).

[38] A. Khor, P. Leung, M. Mohamed, C. Flox, Q. Xu, L. An, R. Wills, J. Morante, A. Shah, Review of zinc-based hybrid flow batteries: from fundamentals to applications, Mater. Today Energy 8 (2018) 80–108, https://doi.org/10.1016/j.mtener.2017.12.012.

[39] L.F. Arenas, A. Loh, D.P. Trudgeon, X. Li, C.P. de León, F.C. Walsh, The characteristics and performance of hybrid redox flow batteries with zinc negative electrodes for energy storage, Renew. Sustain. Energy Rev. 90 (2018) 992–1016, https://doi.org/10.1016/j.rser.2018.03.016.

[40] P.C. Butler, P.A. Eidler, P.G. Grimes, S.E. Klassen, R.C. Miles, Zinc/bromine batteries, in: D. Linden, T.B. Reddy (Eds.), Handbook of Batteries, third ed., McGraw-Hill, New York, 2002, pp. 39.1–39.20.

[41] G.P. Rajarthnam, The Zinc/bromine Flow Battery: Fundamentals and Novel Materials for Technology Advancement, University of Sydney, Faculty of Engineering & Information Technologies, School of Chemical & Biomolecular Engineering, 2016.

[42] D. Bryans, B. McMillan, M. Spicer, A. Wark, L. Berlouis, Complexing additives to reduce the immiscible phase formed in the hybrid ZnBr2 flow battery, J. Electrochem. Soc. 164 (2017) A3342–A3348, https://doi.org/10.1149/2.1651713jes.

[43] H. Lim, A. Lackner, R. Knechtli, Zinc-bromine secondary battery, J. Electrochem. Soc. 124 (1977) 1154–1157, https://doi.org/10.1149/1.2133517.

[44] C. Wang, X. Li, X. Xi, W. Zhou, Q. Lai, H. Zhang, Bimodal highly ordered mesostructure carbon with high activity for Br2/Br− redox couple in bromine based batteries, Nano Energy 21 (2016) 217–227, https://doi.org/10.1016/j.nanoen.2016.01.015.

[45] G. Tomazic, M. Skyllas-Kazacos, Redox Flow Batteries, in: T. Moseley, J. Garche (Eds.), Electrochemical Energy Storage for Renewable Sources and Grid balancing, first ed., Elsevier (Newnes), 2015, pp. 309–336.

[46] S. Biswas, A. Senju, R. Mohr, T. Hodson, N. Karthikeyan, K.W. Knehr, A.G. Hsieh, X. Yang, B.E. Koel, D.A. Steingart, Minimal architecture zinc–bromine battery for low cost electrochemical energy storage, Energy Environ. Sci. 10 (2017) 114–120, https://doi.org/10.1039/C6EE02782B.

[47] H. Kaneko, A. Negishi, K. Nozaki, K. Sato, M. Nakajima, Redox battery. U.S. Patent 5318865, granted, 7 June 1994.

[48] C. Menictas, M. Skyllas-Kazacos, Final Report, SERDF grant, New South Wales Office of Energy, Australia, 1997.

[49] J.N. Noack, C. Cremers, K. Pinkwart, J. Tuebke, Air Breathing Vanadium/oxygen Fuel Cell, Proc. 218th the Electrochemical Society Meeting, The Electrochemical Society, Las Vegas, NV, 2010, 675–675.

[50] S.S. Hosseiny, M. Saakes, M. Wessling, A polyelectrolyte membrane-based vanadium/air redox flow battery, Electrochem. Commun. 13 (2011) 751–754, https://doi.org/10.1016/j.elecom.2010.11.025.

[51] D. Palminteri, Diplomarbeit, Hochschule für Technik und Wirtschaft Karlsruhe, 2011.

[52] J. Noack, T. Berger, J. Tübke, K. Pinkwart, Air-breathing Fuel Cell and Cell Stack for the Oxidation of Ions Using Oxygen, 1 January 2013. WO patent 2013007817A1.

[53] M. Risbud, C. Menictas, M. Skyllas-Kazacos, J. Noack, Vanadium oxygen fuel cell utilising high concentration electrolyte, Batteries 5 (2019) 24–42, https://doi.org/10.3390/batteries5010024.

[54] M. Skyllas-Kazacos, Novel vanadium chloride/polyhalide redox flow battery, J. Power Sources 124 (2003) 299–302, https://doi.org/10.1016/S0378-7753(03)00621-9.

[55] M. Skyllas-Kazacos, New vanadium bromide redox fuel cell, presented at EuroPES2004, Greece (2004).

[56] M. Skyllas-Kazacos, AU2002328660B2, Vanadium/polyhalide Redox Flow Battery, PCT, vol. 23, August 2002. PCT, US7320844B2, (26 August 2002).

[57] M. Skyllas-Kazacos, M. Kazakos, A. Mousa, Improved Vanadium Bromide Battery (Metal Halide Redox Flow Cell), PCT Application, PCT/GB2003/001757, (23 April 2003).

[58] M. Skyllas-Kazacos, N. Kazacos, M. Kazacos, Novel Vanadium Halide Redox Flow Battery. PCT Application, PCT/AU2004/000310, (15 March 2004).

[59] H. Vafiadis, M. Skyllas-Kazacos, Evaluation of membranes for the novel vanadium bromine redox flow cell, J. Membr. Sci. 279 (2006) 394–402, https://doi.org/10.1016/j.memsci.2005.12.028.

[60] C.P. De Leon, A. Frías-Ferrer, J. González-García, D. Szánto, F.C. Walsh, Redox flow cells for energy conversion, J. Power Sources 160 (2006) 716–732, https://doi.org/10.1016/j.jpowsour.2006.02.095.

[61] G. Poon, A. Parasuraman, T.M. Lim, M. Skyllas-Kazacos, Evaluation of N-ethyl-N-methyl-morpholinium bromide and N-ethyl-N-methyl-pyrrolidinium bromide as bromine complexing agents in vanadium bromide redox flow batteries, Electrochim. Acta 107 (2013) 388–396, https://doi.org/10.1016/j.electacta.2013.06.084.

[62] D. Kim, Y. Kim, Y. Lee, J. Jeon, 1, 2-Dimethylimidazole based bromine complexing agents for vanadium bromine redox flow batteries, Int. J. Hydrogen Energy 44 (2019) 12024–12032, https://doi.org/10.1016/j.ijhydene.2019.03.050.

[63] M.C. Tucker, K.T. Cho, F.B. Spingler, A.Z. Weber, G. Lin, Impact of membrane characteristics on the performance and cycling of the Br2–H2 redox flow cell, J. Power Sources 284 (2015) 212–221, https://doi.org/10.1016/j.jpowsour.2015.03.010.

[64] Y. Li, T. Van Nguyen, Core-shell rhodium sulfide catalyst for hydrogen evolution reaction/hydrogen oxidation reaction in hydrogen-bromine reversible fuel cell, J. Power Sources 382 (2018) 152–159, https://doi.org/10.1016/j.jpowsour.2018.02.005.

[65] K.T. Cho, P. Ridgway, A.Z. Weber, S. Haussener, V. Battaglia, V. Srinivasan, High performance hydrogen/bromine redox flow battery for grid-scale energy storage, J. Electrochem. Soc. 159 (2012) A1806–A1815, https://doi.org/10.1149/2.018211jes.

[66] K. Saadi, P. Nanikashvili, Z. Tatus-Portnoy, S. Hardisty, V. Shokhen, M. Zysler, D. Zitoun, Crossover-tolerant coated platinum catalysts in hydrogen/bromine redox flow battery, J. Power Sources 422 (2019) 84–91, https://doi.org/10.1016/j.jpowsour.2019.03.043.

[67] https://www.elestor.nl/technology-the-elestor-solution/about-hydrogen-bromine/.

[68] Elestor electricty storage, Pilot Systems, Elestor project website, 2020. https://www.elestor.nl/projects/. (Accessed 10 September 2020).

[69] E. Peled, A. Blum, A. Aharon, N. Travitsky, Y. Konra, I. Tsamir, V. Zel, K. Saadi, M. Alon, R. Gorenshtein, Energy Storage and Generation Systems US, 2012, 2012/0299384 A1.

[70] N. Singh, E.W. McFarland, Levelized cost of energy and sensitivity analysis for the hydrogen–bromine flow battery, J. Power Sources 288 (2015) 187–198, https://doi.org/10.1016/j.jpowsour.2015.04.114.

[71] M.T. Pope, A. Müller, Polyoxometalate Chemistry from Topology via Self-Assembly to Applications, Springer, Dordrecht, 2001.

[72] S. Francis, Polyoxometalate Chemistry: Some Recent Trends, World Scientific, 2013.

[73] M. Sadakane, E. Steckhan, Electrochemical properties of polyoxometalates as electrocatalysts, Chem. Rev 98 (1998) 219–238, https://doi.org/10.1021/cr960403a.

[74] M. T, Pope Heteropoly and Isopoly Oxometalates, Springer-Verlag, Berlin, 1983.

[75] H.D. Pratt III, N.S. Hudak, X. Fang, T.M. Anderson, A polyoxometalate flow battery, J. Power Sources 236 (2013) 259–264, https://doi.org/10.1016/j.jpowsour.2013.02.056.

[76] H.D. Pratt III, T.M. Anderson, Mixed addenda polyoxometalate “solutions” for stationary energy storage, Dalton Trans. 42 (2013) 15650–15655, https://doi.org/10.1039/C3DT51653A.

[77] Y. Liu, S. Lu, H. Wang, C. Yang, X. Su, Y. Xiang, An aqueous redox flow battery with a tungsten–cobalt heteropolyacid as the electrolyte for both the anode and cathode, Adv. Energy Mater 7 (2017) 1601224–1601229, https://doi.org/10.1002/aenm.201601224.

[78] J.-J. Chen, M.D. Symes, L. Cronin, Highly reduced and protonated aqueous solutions of [P2W18O62]6− for on-demand hydrogen generation and energy storage, Nat. Chem. 10 (2018) 1042–1047, https://doi.org/10.1038/s41557-018-0109-5.

[79] J. Friedl, M.V. Holland-Cunz, F. Cording, F.L. Pfanschilling, C. Wills, W. McFarlane, B. Schricker, R. Fleck, H. Wolfschmidt, U. Stimming, Asymmetric polyoxometalate electrolytes for advanced redox flow batteries, Energy Environ. Sci. 11 (2018) 3010–3018, https://doi.org/10.1039/C8EE00422F.

[80] Jena Batteries, 2020. https://jenabatteries.de/en/. (Accessed 10 September 2020).

[81] F.R. Brushett, M.J. Aziz, K.E. Rodby, On lifetime and cost of redox-active organics for aqueous flow batteries, ACS Energy Lett. 5 (2020) 879–884, https://doi.org/10.1021/acsenergylett.0c00140.

[82] J. Luo, B. Hu, M. Hu, Y. Zhao, T.L. Liu, Status and prospects of organic redox flow batteries toward sustainable energy storage, ACS Energy Lett. 4 (2019) 2220–2240, https://doi.org/10.1021/acsenergylett.9b01332.

[83] B. Hu, Y. Tang, J. Luo, G. Grove, Y. Guo, T.L. Liu, Improved radical stability of viologen anolytes in aqueous organic redox flow batteries, Chem. Commun. 54 (2018) 6871–6874, https://doi.org/10.1039/c8cc02336k.

[84] D.G. Kwabi, Y. Ji, M.J. Aziz, Electrolyte Lifetime in Aqueous Organic Redox Flow Batteries: A Critical Review, Chem. Rev, 2020, https://doi.org/10.1021/acs.chemrev.9b00599.

[85] K. Wedege, E. Drazevic, D. Konya, A. Bentien, Organic redox species in aqueous flow batteries: redox potentials, chemical stability and solubility, Sci. Rep. 6 (2016) 39101–39113, https://doi.org/10.1038/srep39101.

[86] A. Aspuru-Guzik, M.J. Aziz, R.G. Gordon, L. Tong, R. Gómez-Bombarelli, D. Tabor, Theoretical and Experimental Investigation of the Stability Limits of Quinones in Aqueous Media: Implications for Organic Aqueous Redox Flow Batteries, ChemRxiv, 2018, https://doi.org/10.26434/chemrxiv.6990053.v2.

[87] S. Er, C. Suh, M.P. Marshak, A. Aspuru-Guzik, Computational design of molecules for an all-quinone redox flow battery, Chem. Sci. 6 (2015) 885–893, https://doi.org/10.1039/c4sc03030c.

[88] Y. Xu, Y.-H. Wen, J. Cheng, G.-P. Cao, Y.-S. Yang, A study of tiron in aqueous solutions for redox flow battery application, Electrochim. Acta 55 (2010) 715–720, https://doi.org/10.1016/j.electacta.2009.09.031.

[89] B. Huskinson, M.P. Marshak, C. Suh, S. Er, M.R. Gerhardt, C.J. Galvin, X. Chen, A. Aspuru-Guzik, R.G. Gordon, M.J. Aziz, A metal-free organic-inorganic aqueous flow battery, Nature 505 (2014) 195–198, https://doi.org/10.1038/nature12909.

[90] B. Huskinson, M. Marshak, M. Gerhardt, M.J. Aziz, Cycling of a quinone-bromide flow battery for large-scale electrochemical energy storage, ECS Trans 61 (2014) 27–30, https://doi.org/10.1149/06137.0027ecst.

[91] B. Yang, L. Hoober-Burkhardt, F. Wang, G.K. Surya Prakash, S.R. Narayanan, An inexpensive aqueous flow battery for large-scale electrical energy storage based on water-soluble organic redox couples, J. Electrochem. Soc. 161 (2014) A1371–A1380, https://doi.org/10.1149/2.1001409jes.

[92] L. Hoober-Burkhardt, S. Krishnamoorthy, B. Yang, A. Murali, A. Nirmalchandar, G.K.S. Prakash, S.R. Narayanan, A new Michael-reaction-resistant benzoquinone for aqueous organic redox flow batteries,, J. Electrochem. Soc. 164 (2017) A600–A607, https://doi.org/10.1149/2.0351704jes.

[93] A.W. Lantz, S.A. Shavalier, W. Schroeder, P.G. Rasmussen, Evaluation of an aqueous biphenol- and anthraquinone-based electrolyte redox flow battery, ACS Appl. Energy Mater. 2 (2019) 7893–7902, https://doi.org/10.1021/acsaem.9b01381.

[94] B. Yang, A. Murali, A. Nirmalchandar, B. Jayathilake, G.K.S. Prakash, S. R. Narayanan, A durable, inexpensive and dcalable redox flow battery based on iron sulfate and anthraquinone disulfonic acid, J. Electrochem. Soc. 167 (2020), https://doi.org/10.1149/1945-7111/ab84f8.

[95] K. Lin, Q. Chen, M.R. Gerhardt, L. Tong, S.B. Kim, L. Eisenach, A.W. Valle, D. Hardee, R.G. Gordon, M.J. Aziz, Alkaline quinone flow battery, Science 349 (2014) 1529–1532, https://doi.org/10.1126/science.aab3033.

[96] M.A. Goulet, L. Tong, D.A. Pollack, D.P. Tabor, S.A. Odom, A. Aspuru-Guzik, E. E. Kwan, R.G. Gordon, M.J. Aziz, Extending the lifetime of organic flow batteries via redox state management, J. Am. Chem. Soc. 141 (2019) 8014–8019, https://doi.org/10.1021/jacs.8b13295.

[97] D.G. Kwabi, K. Lin, Y. Ji, E.F. Kerr, M.-A. Goulet, D. De Porcellinis, D.P. Tabor, D. A. Pollack, A. Aspuru-Guzik, R.G. Gordon, M.J. Aziz, Alkaline quinone flow battery with long lifetime at pH 12, Joule 2 (2018) 1894–1906, https://doi.org/10.1016/j.joule.2018.07.005.

[98] Y. Ji, M.A. Goulet, D.A. Pollack, D.G. Kwabi, S. Jin, D. Porcellinis, E.F. Kerr, R. G. Gordon, M.J. Aziz, A phosphonate-functionalized quinone redox flow battery at near-neutral pH with record capacity retention rate, Adv. Energy Mater 9 (2019) 1900039–1900045, https://doi.org/10.1002/aenm.201900039.

[99] B. Hu, J. Luo, M. Hu, B. Yuan, T.L. Liu, A pH-neutral, metal-free aqueous organic redox flow battery employing an ammonium anthraquinone anolyte, Angew Chem Int Ed Engl 131 (2019) 16782–16789, https://doi.org/10.1002/ange.201907934.

[100] A. Khataee, E. Dražević, J. Catalano, A. Bentien, Performance optimization of differential pH quinone-bromide redox flow battery, J. Electrochem. Soc. 165 (2018) A3918–A3924, https://doi.org/10.1149/2.0681816jes.

[101] S. Jin, Y. Jing, D.G. Kwabi, Y. Ji, L. Tong, D. De Porcellinis, M.-A. Goulet, D. A. Pollack, R.G. Gordon, M.J. Aziz, A water-miscible quinone flow battery with high volumetric capacity and energy density, ACS Energy Lett 4 (2019) 1342–1348, https://doi.org/10.1021/acsenergylett.9b00739.

[102] J. Luo, A. Sam, B. Hu, C. DeBruler, X. Wei, W. Wang, T.L. Liu, Unraveling pH dependent cycling stability of ferricyanide/ferrocyanide in redox flow batteries, Nanomater. Energy 42 (2017) 215–221, https://doi.org/10.1016/j.nanoen.2017.10.057.

[103] T. Páez, A. Martínez-Cuezva, J. Palma, E. Ventosa, Revisiting the cycling stability of ferrocyanide in alkaline media for redox flow batteries, J. Power Sources 471 (2020) 228453–228458, https://doi.org/10.1016/j.jpowsour.2020.228453.

[104] T.J. Carney, S.J. Collins, J.S. Moore, F.R. Brushett, Concentration-dependent dimerization of anthraquinone disulfonic acid and its impact on charge storage, Chem. Mater. 29 (2017) 4801–4810, https://doi.org/10.1021/acs.chemmater.7b00616.

[105] D.P. Tabor, R. Gómez-Bombarelli, L. Tong, R.G. Gordon, M.J. Aziz, A. Aspuru-Guzik, Mapping the frontiers of quinone stability in aqueous media: implications for organic aqueous redox flow batteries, J. Mater. Chem *A* 7 (2019) 12833–12841, https://doi.org/10.1039/c9ta03219c.

[106] K. Lin, R. Gómez-Bombarelli, E.S. Beh, L. Tong, Q. Chen, A. Valle, A. Aspuru-Guzik, M.J. Aziz, R.G. Gordon, A redox-flow battery with an alloxazine-based organic electrolyte, Nat. Energy 1 (2016) 16102–16109, https://doi.org/10.1038/nenergy.2016.102.

[107] A. Orita, M.G. Verde, M. Sakai, Y.S. Meng, A biomimetic redox flow battery based on flavin mononucleotide, Nat. Commun. 7 (2016) 13230–13237, https://doi.org/10.1038/ncomms13230.

[108] A. Hollas, X. Wei, V. Murugesan, Z. Nie, B. Li, D. Reed, J. Liu, V. Sprenkle, W. Wang, A biomimetic high-capacity phenazine-based anolyte for aqueous

organic redox flow batteries, Nat. Energy 3 (2018) 508–514, https://doi.org/10.1038/s41560-018-0167-3.
[109] Y.Y. Lai, X. Li, K. Liu, W.-Y. Tung, C.-F. Cheng, Y. Zhu, Stable low-cost organic dye anolyte for aqueous organic redox flow battery, ACS Appl. Energy Mater. 3 (2020) 2290–2295, https://doi.org/10.1021/acsaem.9b01735.
[110] C. Wang, X. Li, B. Yu, Y. Wang, Z. Yang, H. Wang, H. Lin, J. Ma, G. Li, Z. Jin, Molecular design of fused-ring phenazine derivatives for long-cycling alkaline redox flow batteries, ACS Energy Lett 5 (2020) 411–417, https://doi.org/10.1021/acsenergylett.9b02676.
[111] C. Zhang, Z. Niu, S. Peng, Y. Ding, L. Zhang, X. Guo, Y. Zhao, G. Yu, Phenothiazine-based organic catholyte for high-capacity and long-life aqueous redox flow batteries, Adv. Mater. 31 (2019) 1901052–1901059, https://doi.org/10.1002/adma.201901052.
[112] T. Liu, X. Wei, Z. Nie, V. Sprenkle, W. Wang, A total organic aqueous redox flow battery employing a low cost and sustainable methyl viologen anolyte and 4-HO-TEMPO catholyte, Adv. Energy Mater 6 (2016), https://doi.org/10.1002/aenm.201501449.
[113] T. Janoschka, N. Martin, M.D. Hager, U.S. Schubert, An aqueous redox-flow battery with high capacity and power: the TEMPTMA/MV system, Angew Chem. Int. Ed. Engl. 55 (2016) 14427–14430, https://doi.org/10.1002/anie.201606472.
[114] J. Luo, B. Hu, C. Debruler, T.L. Liu, A π-conjugation extended viologen as a two-electron storage anolyte for total organic aqueous redox flow batteries, Angew Chem Int Ed Engl 57 (2018) 231–235, https://doi.org/10.1002/anie.201710517.
[115] Y. Liu, M.-A. Goulet, L. Tong, Y. Liu, Y. Ji, L. Wu, R.G. Gordon, M.J. Aziz, Z. Yang, T. Xu, A long-lifetime all-organic aqueous flow battery utilizing TMAP-TEMPO radical, Inside Chem. 5 (2019) 1861–1870, https://doi.org/10.1016/j.chempr.2019.04.021.
[116] B. Hu, C. DeBruler, Z. Rhodes, T.L. Liu, Long-cycling aqueous organic redox flow battery (AORFB) toward sustainable and safe energy storage, J. Am. Chem. Soc. 139 (2017) 1207–1214, https://doi.org/10.1021/jacs.6b10984.
[117] E.S. Beh, D. De Porcellinis, R.L. Gracia, K.T. Xia, R.G. Gordon, M.J. Aziz, A neutral pH aqueous organic–organometallic redox flow battery with extremely high capacity retention, ACS Energy Lett 2 (2017) 639–644, https://doi.org/10.1021/acsenergylett.7b00019.
[118] J. Huang, Z. Yang, V. Murugesan, E. Walter, A. Hollas, B. Pan, R.S. Assary, I. A. Shkrob, X. Wei, Z. Zhang, Spatially constrained organic diquat anolyte for stable aqueous flow batteries, ACS Energy Lett 3 (2018) 2533–2538, https://doi.org/10.1021/acsenergylett.8b01550.
[119] Y. Liu, Y. Li, P. Zuo, Q. Chen, G. Tang, P. Sun, Z. Yang, T. Xu, Screening viologen derivatives for neutral aqueous organic redox flow batteries, ChemSusChem 13 (2020) 2245–2249, https://doi.org/10.1002/cssc.202000381.
[120] J. Luo, B. Hu, C. Debruler, Y. Bi, Y. Zhao, B. Yuan, M. Hu, W. Wu, T.L. Liu, Unprecedented capacity and stability of ammonium ferrocyanide catholyte in pH neutral aqueous redox flow batteries, Joule 3 (2019) 149–163, https://doi.org/10.1016/j.joule.2018.10.010.
[121] Y. Li, Y. Liu, Z. Xu, Z. Yang, Poly (phenylene oxide)-based ion-exchange membranes for aqueous organic redox flow battery, Ind. Eng. Chem. Res. 58 (2019) 10707–10712, https://doi.org/10.1021/acs.iecr.9b01377.
[122] J. Luo, W. Wu, C. Debruler, B. Hu, M. Hu, T.L. Liu, A 1.51 V pH neutral redox flow battery towards scalable energy storage, J. Mater. Chem. A 7 (2019) 9130–9136, https://doi.org/10.1039/c9ta01469a.
[123] W. Liu, Y. Liu, H. Zhang, C. Xie, L. Shi, Y.G. Zhou, X. Li, A highly stable neutral viologen/bromine aqueous flow battery with high energy and power density, Chem. Commun. 55 (2019) 4801–4804, https://doi.org/10.1039/c9cc00840c.
[124] C. DeBruler, B. Hu, J. Moss, J. Luo, T.L. Liu, A sulfonate-functionalized viologen enabling neutral cation exchange, aqueous organic redox flow batteries toward renewable energy storage, ACS Energy Lett 3 (2018) 663–668, https://doi.org/10.1021/acsenergylett.7b01302.
[125] C. DeBruler, B. Hu, J. Moss, X. Liu, J. Luo, Y. Sun, T.L. Liu, Designer two-electron storage viologen anolyte materials for neutral aqueous organic redox flow batteries, Inside Chem. 3 (2017) 961–978, https://doi.org/10.1016/j.chempr.2017.11.001.
[126] T. Janoschka, N. Martin, U. Martin, C. Friebe, S. Morgenstern, H. Hiller, M. D. Hager, U.S. Schubert, An aqueous, polymer-based redox-flow battery using non-corrosive, safe, and low-cost materials, Nature 527 (2015) 78–81, https://doi.org/10.1038/nature15746.
[127] T. Hagemann, M. Strumpf, E. Schröter, C. Stolze, M. Grube, I. Nischang, M. D. Hager, U.S. Schubert, (2,2,6,6-Tetramethylpiperidin-1-yl)oxyl-containing zwitterionic polymer as catholyte species for high-capacity aqueous polymer redox flow batteries, Chem. Mater. 31 (2019) 7987–7999, https://doi.org/10.1021/acs.chemmater.9b02201.
[128] T. Hagemann, J. Winsberg, M. Grube, I. Nischang, T. Janoschka, N. Martin, M. D. Hager, U.S. Schubert, An aqueous all-organic redox-flow battery employing a (2,2,6,6-tetramethylpiperidin-1-yl)oxyl-containing polymer as catholyte and dimethyl viologen dichloride as anolyte, J. Power Sources 378 (2018) 546–554, https://doi.org/10.1016/j.jpowsour.2017.09.007.
[129] Y. Zhu, F. Yang, Z. Niu, H. Wu, Y. He, H. Zhu, J. Ye, Y. Zhao, X. Zhang, Enhanced cyclability of organic redox flow batteries enabled by an artificial bipolar molecule in neutral aqueous electrolyte, J. Power Sources 417 (2019) 83–89, https://doi.org/10.1016/j.jpowsour.2019.02.021.
[130] T. Janoschka, C. Friebe, M.D. Hager, N. Martin, U.S. Schubert, An approach toward replacing vanadium: a single organic molecule for the anode and cathode of an aqueous redox-flow battery, ChemistryOpen 6 (2017) 216–220, https://doi.org/10.1002/open.201600155.
[131] R.A. Potash, J.R. McKone, S. Conte, H.D. Abruña, On the benefits of a symmetric redox flow battery, J. Electrochem. Soc. 163 (2015) A338–A344, https://doi.org/10.1149/2.0971602jes.
[132] J. Winsberg, C. Stolze, S. Muench, F. Liedl, M.D. Hager, U.S. Schubert, TEMPO/Phenazine combi-molecule: a redox-active material for symmetric aqueous redox-flow batteries, ACS Energy Lett 1 (2016) 976–980, https://doi.org/10.1021/acsenergylett.6b00413.
[133] W. Lee, A. Permatasari, B.W. Kwon, Y. Kwon, Performance evaluation of aqueous organic redox flow battery using anthraquinone-2,7-disulfonic acid disodium salt and potassium iodide redox couple, Chem. Eng. J. 358 (2019) 1438–1445, https://doi.org/10.1016/j.cej.2018.10.159.
[134] J. Cao, M. Tao, H. Chen, J. Xu, Z. Chen, A highly reversible anthraquinone-based anolyte for alkaline aqueous redox flow batteries, J. Power Sources 386 (2018) 40–46, https://doi.org/10.1016/j.jpowsour.2018.03.041.
[135] B. Hu, C. Seefeldt, C. DeBruler, T.L. Liu, Boosting the energy efficiency and power performance of neutral aqueous organic redox flow batteries, J. Mater. Chem. A 5 (2017) 22137–22145, https://doi.org/10.1039/c7ta06573f.
[136] E.W. Zhao, T. Liu, E. Jonsson, J. Lee, I. Temprano, R.B. Jethwa, A. Wang, H. Smith, J. Carretero-Gonzalez, Q. Song, C.P. Grey, In situ NMR metrology reveals reaction mechanisms in redox flow batteries, Nature 579 (2020) 224–228, https://doi.org/10.1038/s41586-020-2081-7.
[137] L. Tong, Q. Chen, A.A. Wong, R. Gomez-Bombarelli, A. Aspuru-Guzik, R. G. Gordon, M.J. Aziz, UV-Vis spectrophotometry of quinone flow battery electrolyte for in situ monitoring and improved electrochemical modeling of potential and quinhydrone formation, Phys. Chem. Chem. Phys. 19 (2017) 31684–31691, https://doi.org/10.1039/c7cp05881k.
[138] V. Dieterich, J.D. Milshtein, J.L. Barton, T.J. Carney, R.M. Darling, F.R. Brushett, Estimating the cost of organic battery active materials: a case study on anthraquinone disulfonic acid, Transl. Mater. Res. 5 (2018) 34001–34017, https://doi.org/10.1088/2053-1613/aacb0e.
[139] T. Wu, D. Wang, M. Zhang, J.R. Heflin, R.B. Moore, T.E. Long, RAFT synthesis of ABA triblock copolymers as ionic liquid-containing electroactive membranes, ACS Appl. Mater. Interfaces 4 (2012) 6552–6559, https://doi.org/10.1021/am301662s.
[140] G. Kear, A.A. Shah, F.C. Walsh, Development of the all-vanadium redox flow battery for energy storage: a review of technological, financial and policy aspects, Int. J. Energy Res. 36 (2012) 1105–1120, https://doi.org/10.1002/er.1863.
[141] A.F. Molina-Osorio, A. Gamero-Quijano, P. Peljo, M.D. Scanlon, Membraneless energy conversion and storage using immiscible electrolyte solutions, Curr. Opin. Electrochem. (2020) 100–108, https://doi.org/10.1016/j.coelec.2020.01.013.
[142] J.S. Lee, S. Tai Kim, R. Cao, N.S. Choi, M. Liu, K.T. Lee, J. Cho, Metal–air batteries with high energy density: Li–air versus Zn–air, Adv. Energy Mater 1 (2011) 34–50, https://doi.org/10.1002/aenm.201000010.
[143] R. Ferrigno, A.D. Stroock, T.D. Clark, M. Mayer, G.M. Whitesides, Membraneless vanadium redox fuel cell using laminar flow, J. Am. Chem. Soc. 124 (2002) 12930–12931, https://doi.org/10.1021/ja020812q.
[144] E. Kjeang, R. Michel, D.A. Harrington, N. Djilali, D. Sinton, A microfluidic fuel cell with flow-through porous electrodes, J. Am. Chem. Soc. 130 (2008) 4000–4006, https://doi.org/10.1021/ja078248c.
[145] M.-A. Goulet, E. Kjeang, Co-laminar flow cells for electrochemical energy conversion, J. Power Sources 260 (2014) 186–196, https://doi.org/10.1016/j.jpowsour.2014.03.009.
[146] M.O. Bamgbopa, S. Almheiri, H. Sun, Prospects of recently developed membraneless cell designs for redox flow batteries, Renew. Sustain. Energy Rev. 70 (2017) 506–518, https://doi.org/10.1016/j.rser.2016.11.234.
[147] O.A. Ibrahim, M.-A. Goulet, E. Kjeang, In-situ characterization of symmetric dual-pass architecture of microfluidic co-laminar flow cells, Electrochim. Acta 187 (2016) 277–285, https://doi.org/10.1016/j.electacta.2015.11.081.
[148] J.W. Lee, M.-A. Goulet, E. Kjeang, Microfluidic redox battery, Lab Chip 13 (2013) 2504–2507, https://doi.org/10.1039/c3lc50499a.
[149] E. Kjeang, B.T. Proctor, A.G. Brolo, D.A. Harrington, N. Djilali, D. Sinton, High-performance microfluidic vanadium redox fuel cell, Electrochim. Acta 52 (2007) 4942–4946, https://doi.org/10.1016/j.electacta.2007.01.062.
[150] H.B. Park, K.H. Lee, H.J. Sung, Performance of H-shaped membraneless micro fuel cells, J. Power Sources 226 (2013) 266–271, https://doi.org/10.1016/j.jpowsour.2012.11.003.
[151] P. López-Montesinos, N. Yossakda, A. Schmidt, F. Brushett, W. Pelton, P.J. Kenis, Design, fabrication, and characterization of a planar, silicon-based, monolithically integrated micro laminar flow fuel cell with a bridge-shaped microchannel cross-section, J. Power Sources 196 (2011) 4638–4645, https://doi.org/10.1016/j.jpowsour.2011.01.037.
[152] J. Marschewski, S. Jung, P. Ruch, N. Prasad, S. Mazzotti, B. Michel, D. Poulikakos, Mixing with herringbone-inspired microstructures: overcoming the diffusion limit in co-laminar microfluidic devices, Lab Chip 15 (2015) 1923–1933, https://doi.org/10.1039/C5LC00045A.
[153] J. Marschewski, P. Ruch, N. Ebejer, O.H. Kanan, G. Lhermitte, Q. Cabrol, B. Michel, D. Poulikakos, On the mass transfer performance enhancement of membraneless redox flow cells with mixing promoters, Int. J. Heat Mass Tran. 106 (2017) 884–894, https://doi.org/10.1016/j.ijheatmasstransfer.2016.10.030.
[154] M.-A. Goulet, E. Kjeang, Reactant recirculation in electrochemical co-laminar flow cells, Electrochim. Acta 140 (2014) 217–224, https://doi.org/10.1016/j.electacta.2014.03.092.
[155] P. Navalpotro, J. Palma, M. Anderson, R. Marcilla, A membrane-free redox flow battery with two Immiscible redox electrolytes, Angew Chem Int Ed Engl 56 (2017) 12460–12465, https://doi.org/10.1002/ange.201704318.

[156] P. Navalpotro, N. Sierra, C. Trujillo, I. Montes, J. Palma, R. Marcilla, Exploring the versatility of membrane-free battery concept using different combinations of immiscible redox electrolytes, ACS Appl. Mater. Interfaces 10 (2018) 41246–41256, https://doi.org/10.1021/acsami.8b11581.
[157] M.O. Bamgbopa, Y. Shao-Horn, R. Hashaikeh, S. Almheiri, Cyclable membraneless redox flow batteries based on immiscible liquid electrolytes: demonstration with all-iron redox chemistry, Electrochim. Acta 267 (2018) 41–50, https://doi.org/10.1016/j.electacta.2018.02.063.
[158] P. Navalpotro, C.M. Neves, J. Palma, M.G. Freire, J.A. Coutinho, R. Marcilla, Pioneering use of ionic liquid-based aqueous biphasic systems as membrane-free batteries, Adv. Sci. 5 (2018) 1800576–1800585, https://doi.org/10.1002/advs.201800576.
[159] P. Navalpotro, C. Trujillo, I. Montes, C.M. Neves, J. Palma, M.G. Freire, J. A. Coutinho, R. Marcilla, Critical aspects of membrane-free aqueous battery based on two immiscible neutral electrolytes, Energy Storage Mater 26 (2020) 400–407, https://doi.org/10.1016/j.ensm.2019.11.011.
[160] E. Ventosa, D. Buchholz, S. Klink, C. Flox, L.G. Chagas, C. Vaalma, W. Schuhmann, S. Passerini, J.R. Morante, Non-aqueous semi-solid flow battery based on Na-ion chemistry. P2-type Na x Ni 0.22 Co 0.11 Mn 0.66 O 2–NaTi 2 (PO 4) 3, Chem. Commun. 51 (2015) 7298–7301, https://doi.org/10.1039/c4cc09597a.
[161] T. Páez, A. Martínez-Cuezva, J. Palma, E. Ventosa, Mediated alkaline flow batteries: from fundamentals to application, ACS Appl. Energy Mater. 2 (2019) 8328–8336, https://doi.org/10.1021/acsaem.9b01826.
[162] M. Duduta, B. Ho, V.C. Wood, P. Limthongkul, V.E. Brunini, W.C. Carter, Y. M. Chiang, Semi-Solid lithium rechargeable flow battery, Adv. Energy Mater 1 (2011) 511–516, https://doi.org/10.1002/aenm.201100152.
[163] Y. Yang, G. Zheng, Y. Cui, A membrane-free lithium/polysulfide semi-liquid battery for large-scale energy storage, Energy Environ. Sci. 6 (2013) 1552–1558, https://doi.org/10.1039/C3EE00072A.
[164] F.Y. Fan, W.H. Woodford, Z. Li, N. Baram, K.C. Smith, A. Helal, G.H. McKinley, W. C. Carter, Y.-M. Chiang, Polysulfide flow batteries enabled by percolating nanoscale conductor networks, Nano Lett. 14 (2014) 2210–2218, https://doi.org/10.1021/nl500740t.
[165] Z. Li, K.C. Smith, Y. Dong, N. Baram, F.Y. Fan, J. Xie, P. Limthongkul, W.C. Carter, Y.-M. Chiang, Aqueous semi-solid flow cell: demonstration and analysis, Phys. Chem. Chem. Phys. 15 (2013) 15833–15839, https://doi.org/10.1039/C3CP53428F.
[166] E. Ventosa, O. Amedu, W. Schuhmann, Aqueous mixed-cation semi-solid hybrid-flow batteries, ACS Appl. Energy Mater. 1 (2018) 5158–5162, https://doi.org/10.1021/acsaem.8b01418.
[167] J. Liu, Y. Wang, Preliminary study of high energy density Zn/Ni flow batteries, J. Power Sources 294 (2015) 574–579, https://doi.org/10.1016/j.jpowsour.2015.06.110.
[168] W. Yan, C. Wang, J. Tian, G. Zhu, L. Ma, Y. Wang, R. Chen, Y. Hu, L. Wang, T. Chen, All-polymer particulate slurry batteries, Nat. Commun. 10 (2019) 1–11, https://doi.org/10.1038/s41467-019-10607-0.
[169] V. Presser, C.R. Dennison, J. Campos, K.W. Knehr, E.C. Kumbur, Y. Gogotsi, The electrochemical flow capacitor: a new concept for rapid energy storage and recovery, Adv. Energy Mater 2 (2012) 895–902, https://doi.org/10.1002/aenm.201100768.
[170] E. Ventosa, G. Zampardi, C. Flox, F. La Mantia, W. Schuhmann, J. Morante, Solid electrolyte interphase in semi-solid flow batteries: a wolf in sheep's clothing, Chem. Commun. 51 (2015) 14973–14976, https://doi.org/10.1039/C5CC04767F.
[171] L. Madec, M. Youssry, M. Cerbelaud, P. Soudan, D. Guyomard, B. Lestriez, Surfactant for enhanced rheological, electrical, and electrochemical performance of suspensions for semisolid redox flow batteries and supercapacitors, ChemPlusChem 80 (2015) 396–401, https://doi.org/10.1002/cplu.201402042.
[172] T.S. Wei, F.Y. Fan, A. Helal, K.C. Smith, G.H. McKinley, Y.M. Chiang, J.A. Lewis, Biphasic electrode suspensions for Li-ion semi-solid flow cells with high energy density, fast charge transport, and low-dissipation flow, Adv. Energy Mater 5 (2015) 1500535–1500541, https://doi.org/10.1002/aenm.201500535.
[173] C. Jia, F. Pan, Y.G. Zhu, Q. Huang, L. Lu, Q. Wang, High–energy density nonaqueous all redox flow lithium battery enabled with a polymeric membrane, Sci. Adv. 1 (2015) e1500886–e1500892, https://doi.org/10.1126/sciadv.1500886.
[174] M. Zhou, Y. Chen, Q. Zhang, S. Xi, J. Yu, Y. Du, Y.S. Hu, Q. Wang, Na3V2(PO4)3 as the sole solid energy storage material for redox flow sodium-ion battery, Adv. Energy Mater 9 (2019) 1901188–1901196, https://doi.org/10.1002/aenm.201901188.
[175] Y.G. Zhu, Y. Du, C. Jia, M. Zhou, L. Fan, X. Wang, Q. Wang, Unleashing the power and energy of LiFePO4-based redox flow lithium battery with a bifunctional redox mediator, J. Am. Chem. Soc. 139 (2017) 6286–6289, https://doi.org/10.1021/jacs.7b01146.
[176] Y. Cheng, X. Wang, S. Huang, W. Samarakoon, S. Xi, Y. Ji, H. Zhang, F. Zhang, Y. Du, Z. Feng, Redox targeting-based vanadium redox-flow battery, ACS Energy Lett 4 (2019) 3028–3035, https://doi.org/10.1021/acsenergylett.9b01939.
[177] J. Yu, L. Fan, R. Yan, M. Zhou, Q. Wang, Redox targeting-based aqueous redox flow lithium battery, ACS Energy Lett 3 (2018) 2314–2320, https://doi.org/10.1021/acsenergylett.8b01420.
[178] E. Zanzola, C.R. Dennison, A. Battistel, P. Peljo, H. Vrubel, V. Amstutz, H. H. Girault, Redox solid energy boosters for flow batteries: polyaniline as a case study, Electrochim. Acta 235 (2017) 664–671, https://doi.org/10.1016/j.electacta.2017.03.084.
[179] E. Zanzola, S. Gentil, G. Gschwend, D. Reynard, E. Smirnov, C. Dennison, H. H. Girault, P. Peljo, Solid electrochemical energy storage for aqueous redox flow batteries: the case of copper hexacyanoferrate, Electrochim. Acta 321 (2019) 134704–134714, https://doi.org/10.1016/j.electacta.2019.134704.
[180] M. Zhou, Q. Huang, T.N.P. Truong, J. Ghilane, Y.G. Zhu, C. Jia, R. Yan, L. Fan, H. Randriamahazaka, Q. Wang, Nernstian-potential-driven redox-targeting reactions of battery materials, Inside Chem. 3 (2017) 1036–1049, https://doi.org/10.1016/j.chempr.2017.10.003.
[181] C.D. Wessells, R.A. Huggins, Y. Cui, Copper hexacyanoferrate battery electrodes with long cycle life and high power, Nat. Commun. 2 (2011) 1–5, https://doi.org/10.1038/ncomms1563.
[182] K. Hurlbutt, S. Wheeler, I. Capone, M. Pasta, Prussian blue analogs as battery materials, Joule 2 (2018) 1950–1960, https://doi.org/10.1016/j.joule.2018.07.017.
[183] M. Chamoun, B.J. Hertzberg, T. Gupta, D. Davies, S. Bhadra, B. Van Tassell, C. Erdonmez, D.A. Steingart, Hyper-dendritic nanoporous zinc foam anodes, NPG Asia Mater. 7 (2015) e178–e185, https://doi.org/10.1038/am.2015.32.
[184] R. Wang, D. Kirk, G. Zhang, Effects of deposition conditions on the morphology of zinc deposits from alkaline zincate solutions, J. Electrochem. Soc. 153 (2006) C357–C364, https://doi.org/10.1149/1.2186037.
[185] D.P. Trudgeon, K. Qiu, X. Li, T. Mallick, O.O. Taiwo, B. Chakrabarti, V. Yufit, N. P. Brandon, D. Crevillen-Garcia, A. Shah, Screening of effective electrolyte additives for zinc-based redox flow battery systems, J. Power Sources 412 (2019) 44–54, https://doi.org/10.1016/j.jpowsour.2018.11.030.
[186] P. Leung, C. Ponce-de-León, F. Recio, P. Herrasti, F. Walsh, Corrosion of the zinc negative electrode of zinc–cerium hybrid redox flow batteries in methanesulfonic acid, J. Appl. Electrochem. 44 (2014) 1025–1035, https://doi.org/10.1007/s10800-014-0714-y.
[187] Y. Cheng, H. Zhang, Q. Lai, X. Li, D. Shi, L. Zhang, A high power density single flow zinc–nickel battery with three-dimensional porous negative electrode, J. Power Sources 241 (2013) 196–202, https://doi.org/10.1016/j.jpowsour.2013.04.121.
[188] X. Li, C.P. de León, F. Walsh, R.G. Wills, D. Pletcher, in: Advances in Batteries for Medium and Large-Scale Energy Storage, Elsevier, 2015, pp. 293–315.
[189] D.E. Turney, M. Shmukler, K. Galloway, M. Klein, Y. Ito, T. Sholklapper, J. W. Gallaway, M. Nyce, S. Banerjee, Development and testing of an economic grid-scale flow-assisted zinc/nickel-hydroxide alkaline battery, J. Power Sources 264 (2014) 49–58, https://doi.org/10.1016/j.jpowsour.2014.04.067.
[190] Z. Yuan, Y. Duan, T. Liu, H. Zhang, X. Li, Toward a low-cost alkaline zinc-iron flow battery with a polybenzimidazole custom membrane for stationary energy storage, iScience 3 (2018) 40–49, https://doi.org/10.1016/j.isci.2018.04.006.
[191] Z. Xie, Q. Su, A. Shi, B. Yang, B. Liu, J. Chen, X. Zhou, D. Cai, L. Yang, High performance of zinc-ferrum redox flow battery with Ac−/HAc buffer solution, J. Energy Chem 25 (2016) 495–499, https://doi.org/10.1016/j.jechem.2016.02.009.
[192] S. Selverston, R.F. Savinell, J.S. Wainright, Zinc-iron flow batteries with common electrolyte, J. Electrochem. Soc. 164 (2017) A1069–A1075, https://doi.org/10.1149/2.0591706jes.
[193] F.C. Walsh, C. Ponce de Leon, L. Berlouis, G. Nikiforidis, L.F. Arenas-Martínez, D. Hodgson, D. Hall, The development of Zn–Ce hybrid redox flow batteries for energy storage and their continuing challenges, ChemPlusChem 80 (2015) 288–311, https://doi.org/10.1002/cplu.201402103.
[194] B. Li, Z. Nie, M. Vijayakumar, G. Li, J. Liu, V. Sprenkle, W. Wang, Ambipolar zinc-polyiodide electrolyte for a high-energy density aqueous redox flow battery, Nat. Commun. 6 (2015) 6303–6310, https://doi.org/10.1038/ncomms7303.
[195] A. Orita, M. Verde, M. Sakai, Y. Meng, The impact of pH on side reactions for aqueous redox flow batteries based on nitroxyl radical compounds, J. Power Sources 321 (2016) 126–134, https://doi.org/10.1016/j.jpowsour.2016.04.136.
[196] J. Cheng, L. Zhang, Y.-S. Yang, Y.-H. Wen, G.-P. Cao, X.-D. Wang, Preliminary study of single flow zinc–nickel battery, Electrochem. Commun. 9 (2007) 2639–2642, https://doi.org/10.1016/j.elecom.2007.08.016.
[197] Y. Ito, M. Nyce, R. Plivelich, M. Klein, D. Steingart, S. Banerjee, Zinc morphology in zinc–nickel flow assisted batteries and impact on performance, J. Power Sources 196 (2011) 2340–2345, https://doi.org/10.1016/j.jpowsour.2010.09.065.
[198] L. Zhang, J. Cheng, Y.s. Yang, Y.h. Wen, X.-d. Wang, G.-p. Cao, Study of zinc electrodes for single flow zinc/nickel battery application, J. Power Sources 179 (2008) 381–387, https://doi.org/10.1016/j.jpowsour.2007.12.088.
[199] N.J. Magnani, R.B. Diegle, J.W. Braithwaite, D.M. Bush, J. Freese, A. Akhil, S. Lott, "Exploratory Battery Technology Development and Testing Report for 1989," Sandia National Labs, NM (USA), Albuquerque, 1990.
[200] R. Amirante, E. Cassone, E. Distaso, P. Tamburrano, Overview on recent developments in energy storage: mechanical, electrochemical and hydrogen technologies, Energy Convers. Manag. 132 (2017) 372–387, https://doi.org/10.1016/j.enconman.2016.11.046.
[201] ViZn Energy. GS200® engineered for MW utility scale storage, 2016. https://www.viznenergy.com/product-gs200/. (Accessed 10 September 2020).
[202] K. Gong, X. Ma, K.M. Conforti, K.J. Kuttler, J.B. Grunewald, K.L. Yeager, M. Z. Bazant, S. Gu, Y. Yan, A zinc–iron redox-flow battery under $100 per kW h of system capital cost, Energy Environ. Sci. 8 (2015) 2941–2945, https://doi.org/10.1039/C5EE02315G.
[203] J. Pan, Y. Wen, J. Cheng, J. Pan, S. Bai, Y. Yang, Evaluation of substrates for zinc negative electrode in acid PbO2–Zn single flow batteries, Chin. J. Chem. Eng. 24 (2016) 529–534, https://doi.org/10.1016/j.cjche.2016.01.001.
[204] G. Nikiforidis, L. Berlouis, D. Hall, D. Hodgson, Charge/discharge cycles on Pt and Pt-Ir based electrodes for the positive side of the Zinc-Cerium hybrid redox flow

battery, Electrochim. Acta 125 (2014) 176–182, https://doi.org/10.1016/j.electacta.2014.01.075.
[205] G.-M. Weng, Z. Li, G. Cong, Y. Zhou, Y.-C. Lu, Unlocking the capacity of iodide for high-energy-density zinc/polyiodide and lithium/polyiodide redox flow batteries, Energy Environ. Sci. 10 (2017) 735–741, https://doi.org/10.1039/C6EE03554J.
[206] J. Winsberg, S. Muench, T. Hagemann, S. Morgenstern, T. Janoschka, M. Billing, F.H. Schacher, G. Hauffman, J.-F. Gohy, S. Hoeppener, Polymer/zinc hybrid-flow battery using block copolymer micelles featuring a TEMPO corona as catholyte, Polym. Chem. 7 (2016) 1711–1718, https://doi.org/10.1039/C5PY02036K.
[207] J. Winsberg, T. Janoschka, S. Morgenstern, T. Hagemann, S. Muench, G. Hauffman, J.F. Gohy, M.D. Hager, U.S. Schubert, Poly (TEMPO)/zinc hybrid-flow battery: a novel,"green," high voltage, and safe energy storage system, Adv. Mater. 28 (2016) 2238–2243, https://doi.org/10.1002/adma.201505000.
[208] L. Hruska, R. Savinell, Investigation of factors affecting performance of the iron-redox battery, J. Electrochem. Soc. 128 (1981) 18–25, https://doi.org/10.1149/1.2127366.
[209] A. Dinesh, S. Olivera, K. Venkatesh, M.S. Santosh, M.G. Priya, A.M. Asiri, H. B. Muralidhara, Iron-based flow batteries to store renewable energies, Environ. Chem. Lett. 16 (2018) 683–694, https://doi.org/10.1007/s10311-018-0709-8.
[210] K.L. Hawthorne, J. Wainright, R.F. Savinell, The electrochemical society, Meet. Abstr. (2013), 297–297.
[211] M.C. Tucker, A. Phillips, A.Z. Weber, All-iron redox flow battery tailored for off-grid portable applications, ChemSusChem 8 (2015) 3996–4004, https://doi.org/10.1002/cssc.201500845.
[212] https://www.essinc.com/wp-content/uploads/2020/01/ESSDatasheet_EnergyWarehouse_1-22-20_lores.pdf.
[213] Arpa.e, Iron Flow Battery Energy Storasge Systems (ESS), 2017. https://arpa-e.energy.gov/?q=slick-sheet-project/iron-flow-battery. (Accessed 10 September 2020).
[214] D. Lloyd, E. Magdalena, L. Sanz, L. Murtomäki, K. Kontturi, Preparation of a cost-effective, scalable and energy efficient all-copper redox flow battery, J. Power Sources 292 (2015) 87–94, https://doi.org/10.1016/j.jpowsour.2015.04.176.
[215] L. Sanz, D. Lloyd, E. Magdalena, J. Palma, K. Kontturi, Description and performance of a novel aqueous all-copper redox flow battery, J. Power Sources 268 (2014) 121–128, https://doi.org/10.1016/j.jpowsour.2014.06.008.
[216] D. Lloyd, L. Sanz, Aqueous All-Copper Redox Flow Battery, 2018. US20170033383A1.
[217] D. Lloyd, T. Vainikka, K. Kontturi, The development of an all copper hybrid redox flow battery using deep eutectic solvents, Electrochim. Acta 100 (2013) 18–23, https://doi.org/10.1016/j.electacta.2013.03.130.
[218] S. Schaltin, Y. Li, N.R. Brooks, J. Sniekers, I.F. Vankelecom, K. Binnemans, J. Fransaer, Towards an all-copper redox flow battery based on a copper-containing ionic liquid, Chem. Commun. 52 (2016) 414–417, https://doi.org/10.1039/C5CC06774J.
[219] X. Zhang, X.-G. Wang, Z. Xie, Z. Zhou, Recent progress in rechargeable alkali metal–air batteries, Green Energy & Environment 1 (2016) 4–17, https://doi.org/10.1016/j.gee.2016.04.004.
[220] C.S. Li, Y. Sun, F. Gebert, S.L. Chou, Current progress on rechargeable magnesium–air battery, Adv. Energy Mater 7 (2017) 1700869–1700879, https://doi.org/10.1002/aenm.201700869.
[221] R. McKerracher, C. Ponce de Leon, R. Wills, A. Shah, F.C. Walsh, A review of the iron–air secondary battery for energy storage, ChemPlusChem 80 (2015) 323–335, https://doi.org/10.1002/cplu.201402238.
[222] X. Han, X. Li, J. White, C. Zhong, Y. Deng, W. Hu, T. Ma, Metal–air batteries: from static to flow system, Adv. Energy Mater 8 (2018) 1801396–1801423, https://doi.org/10.1002/aenm.201801396.
[223] W. Yu, W. Shang, P. Tan, B. Chen, Z. Wu, H. Xu, Z. Shao, M. Liu, M. Ni, Toward a new generation of low cost, efficient, and durable metal–air flow batteries, J. Mater. Chem. A 7 (2019) 26744–26768, https://doi.org/10.1039/C9TA10658H.
[224] Q. Liu, Z. Pan, E. Wang, L. An, G. Sun, Aqueous metal-air batteries: fundamentals and applications, Energy Storage Mater (2019), https://doi.org/10.1016/j.ensm.2019.12.011.
[225] X. Chen, A. Shellikeri, Q. Wu, J.P. Zheng, M.a. Hendrickson, E.J. Plichta, A high-rate rechargeable Li-air flow battery, J. Electrochem. Soc. 160 (2013) A1619–A1623, https://doi.org/10.1149/MA2014-01/4/378.
[226] J. Pan, L. Ji, Y. Sun, P. Wan, J. Cheng, Y. Yang, M.J.E.C. Fan, Preliminary study of alkaline single flowing Zn–O_2 battery, Electrochem. Commun. 11 (2009) 2191–2194.
[227] P. Pei, Z. Ma, K. Wang, X. Wang, M. Song, H. Xu, High performance zinc air fuel cell stack, J. Power Sources 249 (2014) 13–20, https://doi.org/10.1016/j.jpowsour.2013.10.073.
[228] Y. Jiang, Y.P. Deng, J. Fu, D.U. Lee, R. Liang, Z.P. Cano, Y. Liu, Z. Bai, S. Hwang, L. Yang, Interpenetrating triphase cobalt-based nanocomposites as efficient bifunctional oxygen electrocatalysts for long-lasting rechargeable Zn–air batteries, Adv. Energy Mater 8 (2018) 1702900–1702910, https://doi.org/10.1002/aenm.201702900.
[229] B. Amunátegui, A. Ibáñez, M. Sierra, M. Pérez, Electrochemical energy storage for renewable energy integration: zinc-air flow batteries, J. Appl. Electrochem. 48 (2018) 627–637, https://doi.org/10.1007/s10800-017-1133-7.
[230] PV Magazine, Zinc-air battery aims for extremely low $45/kWh cost, 2020. https://www.pv-magazine.com/2020/01/27/zinc-air-battery-aims-for-extremely-low-45-kwh-cost/. (Accessed 10 September 2020).
[231] S. Monaco, F. Soavi, M. Mastragostino, Role of oxygen mass transport in rechargeable Li/O2 batteries operating with ionic liquids, J. Phys. Chem. Lett. 4 (2013) 1379–1382, https://doi.org/10.1021/jz4006256.
[232] F. Poli, L.K. Ghadikolaei, F. Soavi, Semi-empirical modeling of the power balance of flow lithium/oxygen batteries, Appl. Energy 248 (2019) 383–389, https://doi.org/10.1016/j.apenergy.2019.04.133.
[233] I. Ruggeri, C. Arbizzani, F. Soavi, A novel concept of semi-solid, Li redox flow air (O2) battery: a breakthrough towards high energy and power batteries, Electrochim. Acta 206 (2016) 291–300, https://doi.org/10.1016/j.electacta.2016.04.139.
[234] I. Ruggeri, C. Arbizzani, F. Soavi, Carbonaceous catholyte for high energy density semi-solid Li/O2 flow battery, Carbon 130 (2018) 749–757, https://doi.org/10.1016/j.carbon.2018.01.056.
[235] https://www.bettery.eu.
[236] P. He, Y. Wang, H. Zhou, A Li-air fuel cell with recycle aqueous electrolyte for improved stability, Electrochem. Commun. 12 (2010) 1686–1689, https://doi.org/10.1016/j.elecom.2010.09.025.
[237] P. Liu, Y.l. Cao, G.R. Li, X.P. Gao, X.P. Ai, H.X. Yang, A solar rechargeable flow battery based on photoregeneration of two soluble redox couples, ChemSusChem 6 (2013) 802–806, https://doi.org/10.1002/cssc.201200962.
[238] N. Yan, G. Li, X. Gao, Solar rechargeable redox flow battery based on Li 2 WO 4/LiI couples in dual-phase electrolytes, J. Mater. Chem. A 1 (2013) 7012–7015, https://doi.org/10.1039/C3TA11360D.
[239] N. Yan, G. Li, X. Gao, Electroactive organic compounds as anode-active materials for solar rechargeable redox flow battery in dual-phase electrolytes, J. Electrochem. Soc. 161 (2014) A736–A741, https://doi.org/10.1149/2.065405jes.
[240] M. Yu, W.D. McCulloch, D.R. Beauchamp, Z. Huang, X. Ren, Y. Wu, Aqueous lithium–iodine solar flow battery for the simultaneous conversion and storage of solar energy, J. Am. Chem. Soc. 137 (2015) 8332–8335, https://doi.org/10.1021/jacs.5b03626.
[241] J. Azevedoa, T. Seippc, J. Burfeindc, C. Sousab, A. Bentiend, J.P. Araújob, A. Mendesa, Unbiased solar energy storage: photoelectrochemical redox flow battery, Nanomater. Energy (2016) 396–405, https://doi.org/10.1016/j.nanoen.2016.02.029.
[242] S. Liao, X. Zong, B. Seger, T. Pedersen, T. Yao, C. Ding, J. Shi, J. Chen, C. Li, Integrating a dual-silicon photoelectrochemical cell into a redox flow battery for unassisted photocharging, Nat. Commun. 7 (2016) 1–8, https://doi.org/10.1038/ncomms11474, 2016.
[243] K. Wedege, J. Azevedo, A. Khataee, A. Bentien, A. Mendes, Direct solar charging of an organic–inorganic, stable, and aqueous alkaline redox flow battery with a hematite photoanode, Angew Chem Int Ed Engl 55 (2016) 7142–7147, https://doi.org/10.1002/anie.201602451.
[244] W.D. McCulloch, M. Yu, Y. Wu, pH-tuning a solar redox flow battery for integrated energy conversion and storage, ACS Energy Lett 1 (2016) 578–582, https://doi.org/10.1021/acsenergylett.6b00296.
[245] W. Li, H.C. Fu, L. Li, M. Cabán-Acevedo, J.H. He, S. Jin, Integrated photoelectrochemical solar energy conversion and organic redox flow battery devices, Angew Chem Int Ed Engl 55 (2016) 13104–13108, https://doi.org/10.1002/anie.201606986.
[246] J.R. McKone, F.J. DiSalvo, H.D. Abruña, Solar energy conversion, storage, and release using an integrated solar-driven redox flow battery, J. Mater. Chem. A 5 (2017) 5362–5372, https://doi.org/10.1039/C7TA00555E.
[247] Q. Cheng, W. Fan, Y. He, P. Ma, S. Vanka, S. Fan, Z. Mi, D. Wang, Photorechargeable high voltage redox battery enabled by Ta3N5 and GaN/Si dual-photoelectrode, Adv. Mater. 29 (2017) 1700312–1700319, https://doi.org/10.1002/adma.201700312.
[248] K. Wedege, D. Bae, E. Dražević, A. Mendes, P.C. Vesborg, A. Bentien, Unbiased, complete solar charging of a neutral flow battery by a single Si photocathode, RSC Adv. 8 (2018) 6331–6340, https://doi.org/10.1039/C8RA00319J.
[249] S. Liao, J. Shi, C. Ding, M. Liu, F. Xiong, N. Wang, J. Chen, C. Li, Photoelectrochemical regeneration of all vanadium redox species for construction of a solar rechargeable flow cell, J. Energy Chem 27 (2018) 278–282, https://doi.org/10.1016/j.jechem.2017.04.005.
[250] W. Li, H.-C. Fu, Y. Zhao, J.-H. He, S. Jin, 14.1% efficient monolithically integrated solar flow battery, Inside Chem. 4 (2018) 2644–2657, https://doi.org/10.1016/j.chempr.2018.08.023.
[251] F. Urbain, S. Murcia-López, N. Nembhard, J. Vázquez-Galván, C. Flox, V. Smirnov, K. Welter, T. Andreu, F. Finger, J.R. Morante, Solar vanadium redox-flow battery powered by thin-film silicon photovoltaics for efficient photoelectrochemical energy storage, J. Phys. D Appl. Phys. 52 (2018) 44001–44009, https://doi.org/10.1088/1361-6463/aaeab9.
[252] S. Murcia-López, M. Chakraborty, N.M. Carretero, C. Flox, J.R. Morante, T. Andreu, Adaptation of Cu (In, Ga) Se 2 photovoltaics for full unbiased photocharge of integrated solar vanadium redox flow batteries, Sustain. Energy Fuels (2020) 1135–1142, https://doi.org/10.1039/C9SE00949C.
[253] Z. Li, M.S. Pan, L. Su, P.-C. Tsai, A.F. Badel, J.M. Valle, S.L. Eiler, K. Xiang, F. R. Brushett, Y.-M. Chiang, Air-breathing aqueous sulfur flow battery for ultralow-cost long-duration electrical storage, Joule 1 (2017) 306–327, https://doi.org/10.1016/j.joule.2017.08.007.
[254] K. Wang, Y. Wu, X. Cao, L. Gu, J. Hu, A Zn–CO2 flow battery generating electricity and methane,, Adv. Funct. Mater. (2020) 1908965–1908973, https://doi.org/10.1002/adfm.201908965.